CSIRO
AUSTRALIA

Synthesis Inversion of Atmospheric CO_2 Using the GISS Tracer Transport Model

I.G. Enting, C.M. Trudinger, R.J. Francey and H. Granek

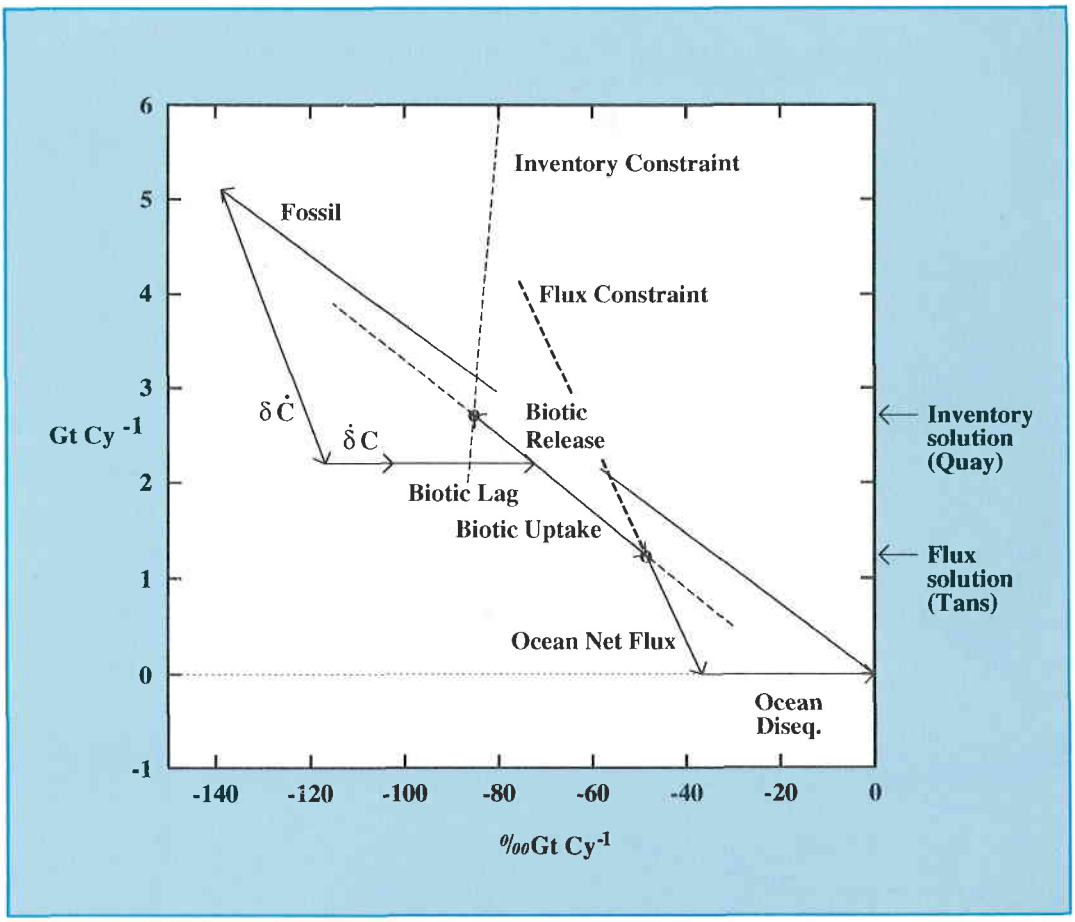

CSIRO DIVISION OF ATMOSPHERIC RESEARCH TECHNICAL PAPER No. 29

ERRATUM

Equations (3), (4a) and (4b) should read

$$w_k = \sum_{\mu=1}^{N'} A_{k\mu}\sigma_\mu \qquad (3)$$

$$w_k = c_k \quad \text{for } k \leq M \qquad (4a)$$

$$w_k = s_{k-M} \quad \text{for } k > M \qquad (4b)$$

Synthesis Inversion of Atmospheric CO_2 Using the GISS Tracer Transport Model

by I.G. Enting, C.M. Trudinger, R.J. Francey and H. Granek

Division of Atmospheric Research Technical Paper No. 29

National Library of Australia Cataloguing-in-Publication Entry

Synthesis Inversion of Atmospheric CO_2 Using the GISS Tracer Transport Model Bibliography.
ISBN 0 643 05251 8
1. Atmospheric carbon dioxide – Measurement. 2. Carbon cycle (Biogeochemistry) – Mathematical models. 3. Atmospheric circulation – Mathematical models.
I. Enting, I.G.. II. CSIRO. Division of Atmospheric Research. (Series: Division of Atmospheric Research Technical Paper; no. 29).
551.51120287

©CSIRO Australia 1993.

Synthesis Inversion of Atmospheric CO_2 Using the GISS Tracer Transport Model

I.G. Enting, C.M. Trudinger, R.J. Francey and H. Granek
CSIRO, Division of Atmospheric Research
Private Bag 1, Mordialloc, Vic 3195, Australia

Contents

Synthesis Inversion of Atmospheric CO_2 Using the GISS Tracer Transport Model

Abstract

The atmospheric CO_2 budget for the period around 1986–7 is estimated using a Bayesian synthesis analysis. The source strengths of a set of industrial, biotic and ocean processes are estimated by matching observed concentrations to modelled concentrations calculated using the GISS three-dimensional tracer transport model. The Bayesian synthesis uses prior estimates of these process strengths to stabilise what is otherwise an ill-conditioned inversion. The analysis gives preliminary estimates of the ranges of uncertainty arising from the inversion.

The inversion uses observations of the concentration and $\delta^{13}C$ of atmospheric CO_2. The ability to estimate uncertainties makes it possible to compare the relative importance of various data items in reducing these uncertainties. The main result is that global totals of oceanic versus biotic exchange are determined primarily by the combined global budgets for CO_2 and $^{13}CO_2$. The atmospheric transport model constrains the regional sources and sinks but these constraints make only a small contribution to reducing the uncertainty in the global budget. Our best estimate of the global net air-sea carbon flux is 1.4 ± 1.0 Gt C y^{-1}. The net carbon storage by the oceans will be some 0.6 Gt C y^{-1} greater than this CO_2 flux due to carbon transported into the oceans by rivers. The corresponding estimate of air-to-biota CO_2 flux is -2.5 ± 0.9 Gt C y^{-1}, implying a net storage of -1.3 Gt C y^{-1} after accounting for carbon lost from the biota via rivers or as CO.

We find that within the range of ≈ 1 Gt C y^{-1} our estimate of air-sea flux is very sensitive to the choice of data that are fitted. This confirms the appropriateness of our formal error estimates that are based on *a priori* statistics. These large uncertainties mean that our budget estimates must be regarded as preliminary and indicate the need for a refined statistical analysis of the observational data to assess their representativeness.

We present a simple preliminary study of oxygen distributions. The results indicate that, once the CO_2 distribution is fitted, the spatial gradient of oxygen does not give significant additional discrimination between alternative carbon budgets and that the long-term trend of atmospheric oxygen will make the greatest contribution to resolving carbon budgets.

1. Introduction

The atmospheric budgets of the major greenhouse gases are subject to very considerable uncertainty (see for example IPCC, 1990). This uncertainty in the budget leads to corresponding uncertainties in projections of the future concentrations to be expected from various possible release scenarios and thus complicates any choices regarding emission-reduction strategies. Clarification of the atmospheric carbon budget is therefore highly desirable.

For CO_2 and CH_4 most recent estimates of the atmospheric budget have been based on the use of atmospheric transport modelling to interpret the space-time distributions of concentrations in terms of the space-time distributions of sources and sinks (Keeling et al., 1989b; Tans et al., 1990a; Sarmiento and Sundquist, 1992; Fung et al., 1991). The principle is that, to the extent that the spatial distribution of sources and sinks can be deduced from observations, the location will act as a constraint on the possible processes.

The determination of surface sources and sinks from observations of surface concentrations is a poorly-determined inverse problem (Newsam and Enting, 1988; Enting and Newsam, 1990). As such, direct estimates of sources are subject to arbitrarily large errors arising from errors in any or all of the observations, the transport model or the inversion technique. In general, meaningful estimates can only be obtained in the context of a set of prior constraints.

A range of inversion calculations estimating the spatial distribution of sources of trace gases have been performed: for CO_2 by Enting and Mansbridge (1989, 1991), Tans et al. (1989, 1990a), Keeling et al. (1989b), Taylor (1989), Law et al. (1992); for CH_4 by Fung et al. (1991), Brown (1992, 1993) and for CFCs by Hartley (1992), Hartley and Prinn (1992, 1993).

Most of the two-dimensional inversions have used some form of surface mass balance to deduce sources from concentrations (Enting and Mansbridge, 1989, 1991; Tans et al., 1989; Brown, 1992, 1993). This method does not readily generalise to three-dimensional models because the observational data do not adequately specify the full surface concentration field — see however some preliminary studies by Law et al. (1992). The solutions of such 'mass-balance' inversions are generally stabilised by assuming some smoothness properties of the concentrations and sources. Most of the inversions using three-dimensional transport models have been based on some sort of synthesis approach (Keeling et al., 1989b; Tans et al., 1990a; Fung et al., 1991). The method involves seeking a linear combination of source/sink processes such that the corresponding linear combination of their calculated responses matches the observational data. In synthesis calculations the solutions are stabilised by the assumptions about the spatial distributions of the source components.

We present a new synthesis estimate of the atmospheric CO_2 budget, applying to 1986–1987. Particular features of our calculation are: the use of a Bayesian estimation procedure, and an attempt to obtain systematic (and realistic) estimates of the uncertainties in the estimated budget. Our error analysis is preliminary — a full error analysis would include the effects of uncertainties in spatial distributions (we discuss some possibilities in Section 6 but do not present any results) and the effects of transport model error (which we have been unable to assess because a suitable methodology has not been developed).

The outline of the remainder of this report is as follows: Section 2 describes the inversion technique that we adopted, firstly in general terms and then in terms of the specific way in which the model calculations are combined to give estimates of the source/sink strengths. Section 3 describes the way in which the source processes are divided into distinct components for use in the synthesis analysis. It gives the values of the scale factors involved in the various atmospheric responses to the processes and in addition gives the prior estimates required by the Bayesian formalism. Section 4 describes the observational data used in the studies. The results of the inversions are presented in Section 5. Section 6 discusses several possible extensions to the calculations, particularly extensions to the error analysis. Section 7 concludes the body of the report, discussing the implications of our results for understanding the global carbon cycle and considering the areas in which a refinement of the present studies seem possible and desirable. The details of the transport model are given in Appendix A. Appendix B describes the use of a simple biotic model to estimate the amount of isotopic disequilibrium between the atmosphere and the terrestrial biota. Appendix C defines our notation.

2. Inversion techniques

2a Generic formalism

The synthesis process seeks to estimate the strengths, σ_μ, of N source/sink processes by comparing M observed concentrations, c_j, to responses calculated using an atmospheric transport model. If the model response for observation j to a source μ of unit strength is $T_{j\mu}$ then the fit is made on the assumption that

$$c_j = \sum T_{j\mu}\sigma_\mu + \text{observational noise} \tag{1}$$

In the Bayesian formalism, the fit is constrained to take account of prior estimates, s_μ, of the source strengths. In this report we consider only least squares fits. This corresponds to assuming independent normal distributions for the prior estimates and the data. This Bayesian inversion is obtained by minimising

$$\Theta = \sum_{j=1}^{M}(c_j - \sum_{\mu=1}^{N'} T_{j\mu}\sigma_\mu)^2/u_j^2 + \sum_{\mu=1}^{N}(\sigma_\mu - s_\mu)^2/v_\mu^2 \tag{2}$$

where u_j is the standard deviation of the observational noise of c_j and v_μ is the standard deviation of the prior estimate s_μ. Taking $N' > N$ allows for some additional 'pseudo-sources' which we exclude from the fit to the prior estimates (see below).

Our implementation solves the minimisation problem as a weighted least-squares solution of the equations

$$v_k = \sum_{\mu=1}^{N'} A_{k\mu}\sigma_\mu \qquad \text{for } k = 1 \text{ to } M+N \tag{3}$$

with the 'data' defined as:

$$v_k = c_k \qquad \text{for } k \leq M \tag{4a}$$

$$v_k = s_{k-M} \qquad \text{for } k > M \tag{4b}$$

with weights:

$$d_k = u_k \qquad \text{for } k \leq M \tag{5a}$$

$$d_k = v_{k-M} \qquad \text{for } k > M \tag{5b}$$

and responses:

$$A_{k\mu} = T_{k\mu} \qquad \text{for } k \leq M \tag{6a}$$

$$A_{k\mu} = \delta_{k-M,\mu} \qquad \text{for } k > M \tag{6b}$$

The equations are solved using a modified version of routine SVDFIT (and the routines which it calls) from Press et al. (1986). This produces estimates $\hat{\sigma}_\mu$ of the source strengths. The routine SVDVAR is used to calculate the covariance matrix $V_{\mu\eta}$ for these estimates.

2b Implementation

In order to apply the formalism from the previous section in a synthesis study, we need to be more specific about the types of data that are fitted. For each j in the range 1 to M we define 3 indicator functions:

$\nu(j)$ — which takes values 1, 2 or 3 to specify whether the data item refers to CO_2, $^{13}CO_2$ or O_2 respectively;

$\rho(j)$ — which specifies the location of the observation;

$\omega(j)$ — which specifies the frequency of the time variation.

The frequency index takes values 0 for the annual mean, -1 and $+1$ for the sine and cosine of $2\pi t$ and -2 and $+2$ for the sine and cosine of $4\pi t$. The special value $\omega(j) = 10000$ refers to the global trend. In this case $\rho(j)$ is undefined.

The trend data have:

$$T_{j\mu} = G_{\nu(j)}(\mu) \qquad \text{if } \omega(j) = 10000 \tag{7a}$$

where the factors $G_\nu(\mu)$ specify the contribution of source μ to the trend in constituent ν. The $G_\nu(\mu)$ are listed in Table 1, with μ as a row index.

Another 'special case' involves the need to estimate a global mean offset for the concentration of each constituent. These offsets are included in the formalism as 'pseudo-sources' contributing to the data with a factor:

$$T_{j\mu} = 1 \qquad \text{if } \omega(j) = 0 \text{ and } \mu \text{ is the 'pseudo-source' for constituent } \nu(j) \tag{7b}$$

The pseudo-sources for CO_2, $^{13}CO_2$ and O_2 are given indices $\mu = N+1, N+2, N+3$. Thus the sum in (3) runs from 1 to $N' = N + 3$.

Each of the 'real' sources has a characteristic space-time distribution which in turn gives a characteristic space-time distribution in the atmospheric concentration. We define an index $\phi(\mu)$ to refer to the space-time distributions for process μ since, in a few cases, several processes have the same distribution (which implies that they can *only* be distinguished on the basis of distinctions between the constituents). The distributions of responses are denoted $R_{\rho\omega\phi}$ and so

$$T_{j\mu} = R_{\rho(j)\omega(j)\phi(\mu)} F_{\nu(j)}(\mu) \qquad \text{for } \omega(j) \in [-2, 2] \text{ and } \mu \leq N \tag{7c}$$

The factors $F_\nu(\mu)$ specify the relative responses for each of the constituents and are listed in Table 1.

In the present study, we have fitted each observational record to the model concentration for the cell containing the observing site. We have not attempted any refined estimation based on interpolation between grid-point values, although such an extension could be readily incorporated within the formalism described here. Similarly, we have not adopted the approach used by Fung et al. (1991) of fitting data to neighbouring grid cells for coastal sites where the model will have a source that acts on the whole grid cell (with reduced strength) while the data will generally be selected for onshore transport. (We have tested such 'corrections' and found that the changes in the solution are small compared to the range of uncertainty.)

Figure 1 gives a schematic representation of the information flow in our analysis.

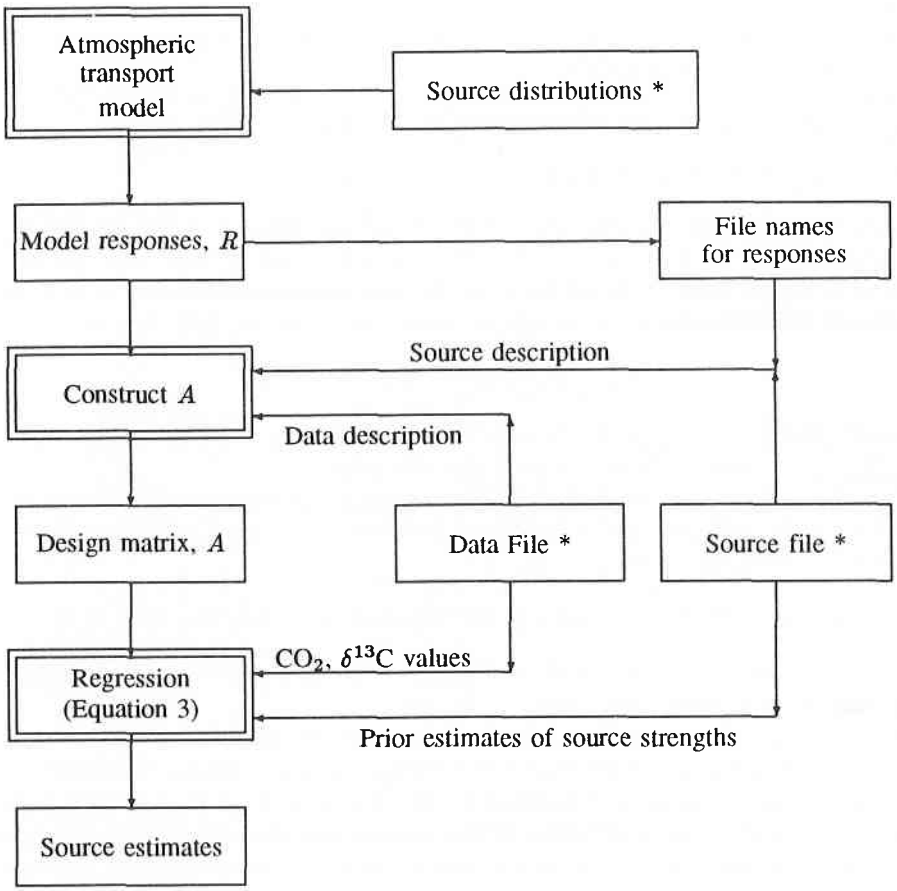

Figure 1: Information flow in the synthesis analysis. Double boxes denote processing, single boxes denote information. The source distributions (described in Section 3b) are used in the GISS transport model to produce sets of model responses, $\boldsymbol{R}$. These are combined with source specifications ($\boldsymbol{F}(\mu)$, $\boldsymbol{G}(\mu)$ and $\boldsymbol{\phi}(\mu)$ from Table 1) and data specifications ($\nu(j)$, $\rho(j)$ and $\omega(j)$) (Section 4) to produce the design matrix $\boldsymbol{A}$. The final stage of processing takes the prior estimates of the sources ($\boldsymbol{s}_\mu$ and $\boldsymbol{v}_\mu$ from Section 3e) and the data values (c_j and u_j from Section 4) to produce source estimates $\hat{\sigma}_\mu$ and the covariance matrix V. The *'s denote input files.

2c Units and normalisations

- The observational data are expressed in ppmv (parts per million by volume) for CO_2 and O_2, except for the trend terms which are in ppmv per year;
- The $^{13}CO_2$ data are expressed as a ^{13}C anomaly, X, as defined below with units of ‰ppmv.
- The pseudo-sources defining global mean concentrations are expressed in the units of the corresponding concentrations, for convenience.
- Real sources, σ_μ, are in Gt C y^{-1} (gigatonnes of carbon per year), specifying the annual mean source strength, except for the seasonal component. We choose the sign convention that sources to the atmosphere are positive.
- The calculated responses are in units of ppmv of CO_2 per Gt C y^{-1} except for the seasonal biotic flux. This means that the CO_2 scale factors $F_1(\mu)$ will generally be equal to 1. The other $F_\nu(\mu)$ convert the CO_2 responses to responses for ^{13}C anomalies and O_2 concentrations.
- The seasonal biotic source is expressed as a numerical multiple of the prior source distribution which is based on the work of Fung et al. (1983) and which has a NPP of 45.6 Gt C y^{-1}.
- The gross fluxes between atmosphere and biota and atmosphere and oceans are expressed as Gt C y^{-1} for consistency, even though the gross flux terms do not appear in the carbon budget, being required only in calculating the effect of isotopic disequilibrium.

Isotopic compositions are frequently expressed in terms of the 'δ' notation that expresses the amount by which an isotopic ratio differs from a standard. For $^{13}CO_2$ the definition is

$$\delta^{13}C = [^{13}C{:}^{12}C_{\text{sample}}/^{13}C{:}^{12}C_{\text{standard}} - 1] \times 1000 \qquad (8a)$$

in units of per mil (denoted ‰). We denote the standard $^{13}C{:}^{12}C$ ratio by r_{standard}. (Its measured value of 0.0112372 is not explicitly needed.)

The ^{13}C anomaly used in the calculation is

$$X = ([^{13}C]/R_{\text{ref}} - [C]) \times 1000 \qquad (8b)$$

where R_{ref} is a reference $^{13}C{:}C$ ratio. X acts as a conservative tracer. If we used $R_{\text{ref}} = R_{\text{standard}}$ (where $R_{\text{standard}} = r_{\text{standard}}/(1 + r_{\text{standard}})$ is the standard $^{13}C{:}C$ ratio for a $\delta^{13}C$ of zero), then X would be equal (to a very good approximation) to $[C] \times \delta^{13}C$. This choice of anomaly definition is used in Section 4d when discussing global budgets. For the purposes of the inversion calculation however, rather than choose R_{ref} to correspond to a $\delta^{13}C$ of zero, we choose R_{ref} to correspond to a $\delta^{13}C$ of -8, close to the observed atmospheric mean. With this definition, we have, to a good approximation

$$X = (\delta^{13}C + 8)[C] \qquad (8c)$$

The approximation in our calculations arises from the fact that the $\delta^{13}C$ quantification of isotopic variations is expressed in terms of $^{13}C{:}^{12}C$ ratios while the present calculations

need ^{13}C:C ratios. We assume that all the ratios are sufficiently close to the standard ratio 0.0112372 that we can convert from ^{13}C:^{12}C ratios (denoted by lower case 'r') to ^{13}C:C ratios (denoted by upper case 'R') by multiplying by $1/(1 + r_{\mathrm{standard}})$. We shall use this approximation without further comment.

The reason for the choice of offset in defining X can be seen when we consider the trend in X. We have:

$$\frac{d}{dt}X = (\delta^{13}\mathrm{C} + 8)\frac{d}{dt}[\mathrm{C}] + [\mathrm{C}]\frac{d}{dt}\delta^{13}\mathrm{C} \tag{9}$$

By choosing R_{ref} so that the factor $(\delta^{13}\mathrm{C} + 8)$ is close to zero, the uncertainty in the trend in X is almost entirely due to the uncertainty in $\frac{d}{dt}\delta^{13}\mathrm{C}$. Similarly, for seasonal and spatial variations about the mean atmospheric isotopic composition, the uncertainties in X can be treated as due solely to the uncertainties in the δ^{13}C measurements. This simplifies the calculations of the effect of these uncertainties on the estimated sources.

The CO_2 conversion factor 0.471 ppmv per Gt C is the ratio of the number of moles ($\frac{1}{12.01} \times 10^{15}$) in a gigatonne of carbon to the number of moles of dry air in the atmosphere (a mass of 512.4×10^{19} g, Trenberth, 1981, divided by a mean molecular weight of 28.9644) with the ratio multiplied by 10^6 to convert the mixing ratio to ppmv.

2d Supplementary analysis

Beyond the regression analysis that forms the basis of our inversion technique there are three additional calculations that assist in the interpretation of the results and which we have implemented as routine parts of the inversion calculation.

The first is the ability to look at the covariances of linear combinations of the data. Perhaps the most obvious example is the relation between the estimates of summed biotic exchange and summed ocean exchange. The formalism is straightforward. For a set of K quantities defined by the linear combinations $x_\beta = \sum_\mu q_{\beta\mu}\sigma_\mu$, the covariance of x_β and x_γ is given by $\sum_{\mu\eta} V_{\mu\eta} q_{\beta\mu} q_{\gamma\eta}$.

Secondly, we include the capability of calculating the residuals $D_j = c_j - \sum_\mu A_{j\mu}\hat{\sigma}_\mu$ and the normalised residuals D_j/u_j.

The final related feature is the ability to look at the concentration distributions implied by the inversion. In particular we consider the zonal means. For each response calculated using the GISS model, we have included the zonal mean response. These zonal mean responses are then combined using the solution coefficients, $\hat{\sigma}_\mu$, and the weights, F_ν, to give zonal mean distributions of concentration, ^{13}C anomaly and oxygen. The anomaly distribution is combined with the concentration to produce the δ^{13}C distribution.

3. Source components

Process	Distrib.	F_1	F_2	F_3	G_1	G_2	G_3	Prior	sd
Mean CO_2	Uniform	1	0	0	0	0	0	n.a.	n.a.
Mean $^{13}CO_2$	Uniform	0	1	0	0	0	0	n.a.	n.a.
Mean O_2	Uniform	0	0	1	0	0	0	n.a.	n.a.
Fossil	Fossil	1	−19	−1.41	0.471	−8.95	−0.664	5.3	0.3
Land-use	Land-use	1	−17	−1.05	0.471	−8.01	−0.495	2.2	1.0
Bio. uptake	Bio-uptake	1	−17	−1.05	0.471	−8.01	−0.495	−2.8	1.0
CO oxid.	CO	1	−17	−0.5*	0.471	−8.01	−0.471	0.9	0.2
Seasnl. bio.	Season	1	−17	−1.05	0	0	0	1.0	0.5
Bio. diseq	Bio-release	0	0.30	0	0	0.141	0	100	50
n:Atlant(B)	Atlant(B)	1	−1.70	0	0.471	−0.80	0	−0.2	0.5
n:Pacif(B)	Pacif(B)	1	−1.70	0	0.471	−0.80	0	0.2	0.5
n:Atlant(N)	Atlant(N)	1	−1.45	0	0.471	−0.68	0	−0.3	1.0
n:Pacif(N)	Pacif(N)	1	−1.45	0	0.471	−0.68	0	−0.3	1.0
n:Equat.	Equatorial	1	−1.45	0	0.471	−0.68	0	1.7	1.5
n:Atlant(S)	Atlant(S)	1	−1.45	0	0.471	−0.68	0	−0.5	1.0
n:Pacif(S)	Pacif(S)	1	−1.45	0	0.471	−0.68	0	−1.0	1.5
n:Indian(S)	Indian(S)	1	−1.45	0	0.471	−0.68	0	−0.7	1.0
n:South.	Southern	1	−1.45	0	0.471	−0.68	0	−0.2	1.0
g:Atlant(B)	Atlant(B)	0	−0.94	0	0	−0.44	0	2.7	1.4
g:Pacif(B)	Pacif(B)	0	−1.08	0	0	−0.51	0	2.5	1.3
g:Atlant(N)	Atlant(N)	0	0.67	0	0	0.32	0	5.1	2.6
g:Pacif(N)	Pacif(N)	0	0.32	0	0	0.15	0	8.7	4.4
g:Equat.	Equatorial	0	1.53	0	0	0.72	0	17.2	8.6
g:Atlant(S)	Atlant(S)	0	0.43	0	0	0.20	0	4.0	2.0
g:Pacif(S)	Pacif(S)	0	0.74	0	0	0.35	0	8.4	4.2
g:Indian(S)	Indian(S)	0	0.46	0	0	0.21	0	5.7	2.9
g:South.	Southern	0	−1.50	0	0	−0.71	0	22.3	11.0

Table 1: Summary of source components used in the synthesis studies. Regional suffices for oceans refer to Far north (B for boreal), North (N) and South (S). Prefices 'n:' and 'g:' refer to the contributions of net air-sea flux and gross air-sea flux (through isotopic disequilibrium) respectively. The effect of CO on the spatial distributions of oxygen (marked with '*') is discussed in the text.

3a Summary

Table 1 summarises the source components that we use in the synthesis studies. Each line represents a distinct process with a source strength to be estimated. (The first three lines are 'pseudo sources' — we need to fit these quantities as part of the estimation process even though they are not of interest.) Each process, μ, is characterised by a specified space-time distribution of surface flux. Column 2 specifies the distribution for each process. The details of these distributions are given in Section 3b below.

Each process will have a characteristic response factor, $F_\nu(\mu)$, for CO_2, the ^{13}C anomaly and for O_2 (denoted by $\nu = 1, 2, 3$). These factors are listed in columns 3 to 5 and are

discussed in connection with each process in Section 3c below. Columns 6 to 8 give the response factors $G_\nu(\mu)$ for the three trends. The final 2 columns give the prior estimate, s_μ, and standard deviation, v_μ, as required for the Bayesian formalism. The basis of the choices made for these values is described in Section 3e below.

3b Space-time distributions

The GISS tracer-transport model (see Appendix A for further details) is used to simulate the space-time distribution of CO_2 concentrations due to a number of source components. In performing the model runs, we are interested in the spatial and temporal distributions of the source components, rather than the actual magnitudes. To simplify calculations, the annual global sources are scaled to 1 Gt C y^{-1} for all source components except the seasonal biospheric source which has zero annual mean net source. Taking each source component separately, the model is run for four simulated years from an initial zero concentration in order to let a stable north-south gradient develop, and concentrations from the fourth year are recorded for analysis. The detrended series for year 4 from each site are fitted with Fourier components to define the responses $R_{\tau\phi\nu}$ for the various space-time distributions of sources.

Fossil Carbon

The fossil fuel source is based on estimates of the global distribution of CO_2 emissions due to fossil fuel burning, and cement production, for 1980 (Marland et al., 1985). The source is given on a 5° × 5° grid and re-mapped onto the tracer model's 8° × 10° grid. Seasonal variation is incorporated into the source by distributing the annual release totals throughout the year using monthly fossil fuel CO_2 emissions for 1982. These are given for six major world regions by Rotty (1987).

Oceans

The oceans are divided into 9 regions as shown in Figure 2. Each region is assumed to be essentially uniform. The characteristics are summarised in Table 2. The regions are defined mainly to reflect different temperature ranges, as many of the variables affecting total carbon and isotope fluxes are either temperature-dependent or follow similar patterns to the temperature. Sources in each of the ocean regions are modelled separately. The tracer model was run with a source arbitrarily set at 1 Gt C y^{-1} and distributed evenly throughout each ocean region. No seasonal variation in the source is considered in this study.

Biotic uptake and release

The distribution of net primary production (NPP) or CO_2 uptake by plants is used in calculating fluxes between the atmosphere and the biosphere. The NPP distribution is calculated using source estimates from Pearman and Hyson (1986) for 10 different vegetation types, combined with vegetation maps at 1° × 1° from Matthews (1985). The annual NPP in each model cell is calculated as the sum of contributions from each of the 1° × 1° cells in the model cell. The global NPP derived in this way is 45.6 Gt C y^{-1}.

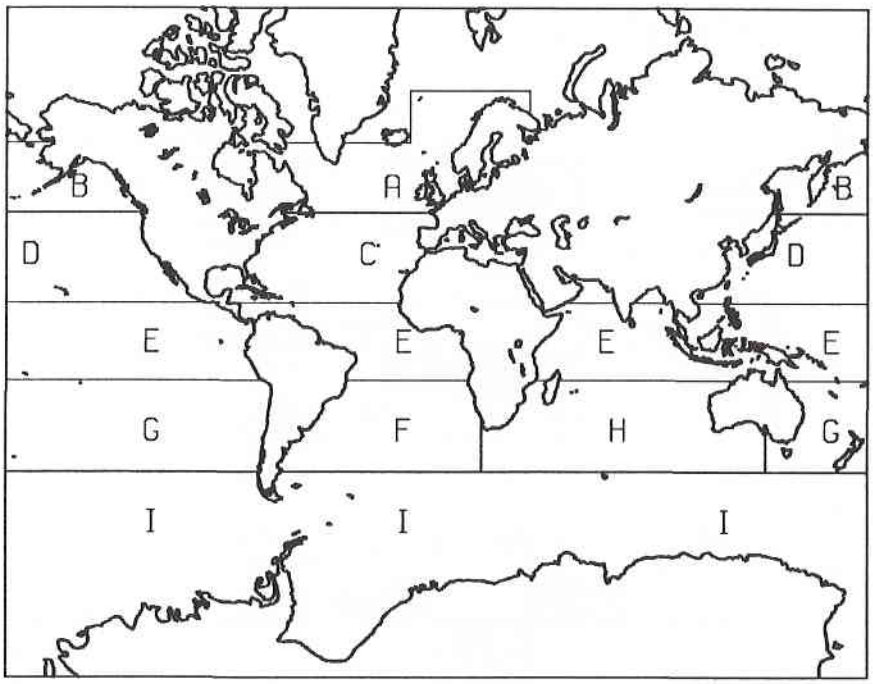

Figure 2: Locations of our 9 ocean regions: A = Far north Atlantic, B = Far north Pacific, C= North Atlantic, D = North Pacific, E = Equatorial, F = South Atlantic, G = South Pacific, H = South Indian, I= Southern.

The spatial distribution of NPP is used in the simulation of both uptake and release by the biota. The uptake and release components have different seasonal variations. Uptake by the biota is concentrated in the summer months when most growth occurs while release is spread more evenly through the year. The seasonal variations of uptake and release are taken to be functions of latitude and are based on the curves used by Fung et al. (1983) which were taken from the thesis of Azevedo (1982). We include an additional annual cycle for latitudes greater than 70°. We assume that uptake is concentrated over 2 summer months and release over 6 months centred in summer. The time variations of uptake and release for various latitudes are shown in Figure 3.

The standard runs use only the two *uptake* and *release* distributions. The *uptake* distribution is used for the 'fertilisation' term and the *release* distribution is used for the biotic disequilibrium. The difference between release and uptake defines the *seasonal* distribution.

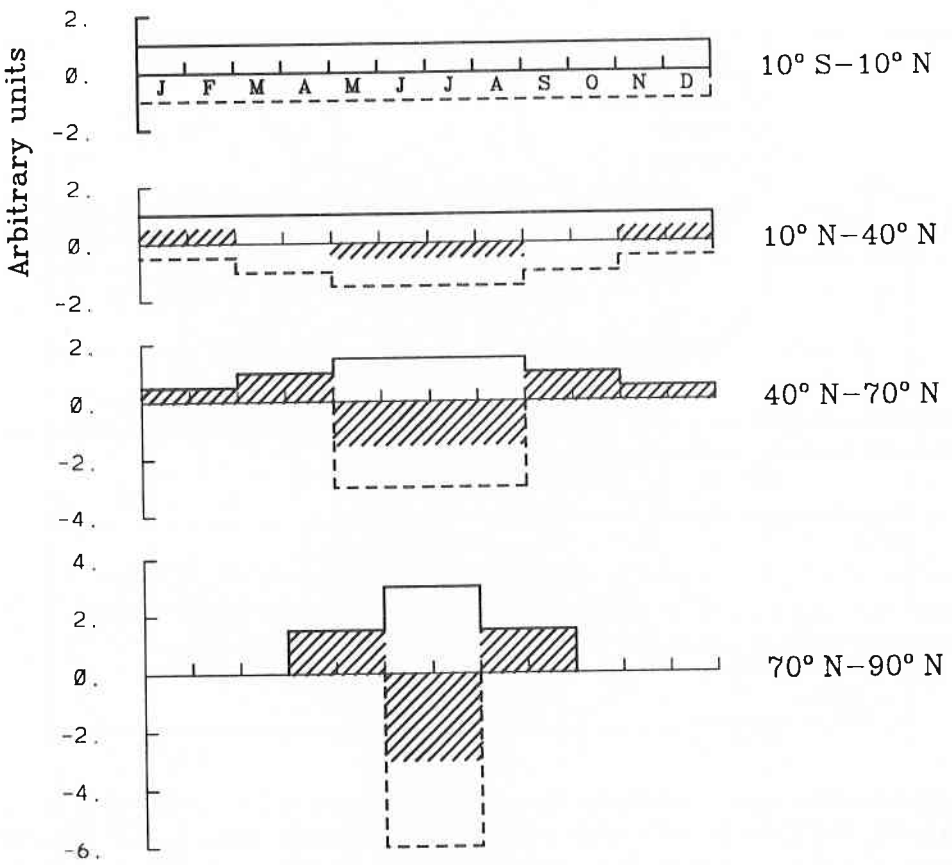

Figure 3: Time variation of release (solid) and uptake (dashed) of CO_2 by the terrestrial biota. Shaded regions indicate net fluxes. Based on Azevedo (1982). Curves are shifted by 6 months for the southern hemisphere.

Land-use changes

The source of carbon due to land-use changes (the net effect of clearing of forests for agriculture, forest regrowth etc.) is discussed in Houghton et al. (1987). The estimated net release of carbon to the atmosphere in 1980 was 1.791 Gt C y^{-1}, and is given by major world region. We distribute these totals within each region in proportion to the spatial distribution of net primary productivity described above, but redefine the seasonality. A peak of 20% in the source is imposed during the 3 driest months of the year in the tropics to reflect increased biomass burning in the dry season. Rainfall statistics are used to determine which are the driest months for each region.

CO oxidation

This source differs from the others in that it is spread throughout the entire depth of the troposphere. The source is taken as uniform in time and longitude and vertically uniform through the troposphere. The latitudinal distribution (which we take from Enting and Mansbridge, 1991) peaks in the tropics reflecting the role of photochemistry in the oxidation of CO.

3c Conversions

In analysing the atmospheric carbon budget, we need to consider 3 distinct quantities associated with carbon reservoirs:

- CO_2 fluxes to or from the atmosphere;
- Carbon fluxes to or from the atmosphere;
- Carbon loss or storage by the reservoir.

The distinctions arise in two ways. CO_2 fluxes differ from carbon fluxes due to fluxes of other gases, mainly CO and CH_4, together with organic compounds that are rapidly oxidised to CO. Carbon fluxes to and from the atmosphere differ from carbon storage because of other inter-reservoir transfers. The most notable of these is the transport of carbon from the terrestrial biota into the oceans via rivers.

Given these distinctions it is important to be clear about which type of quantity is being estimated. *Inversions of atmospheric CO_2 data give estimates of CO_2 fluxes.*

By analysing the processes that lead to these distinctions, we can estimate the exchange that needs to be added to *convert* one type of quantity to the other. We advocate the use of the term *conversion* from one type of quantity to another rather than the term *correction* which has often been used. It is not that any of the three quantities is 'wrong' (and thus in need of correction) but rather that three different quantities are involved.

The conversion terms need to be taken into account both in the interpretation of results from inversion calculations and in the determination of prior fluxes for the Bayesian estimation.

Sarmiento and Sundquist (1992) pointed out the significance of the natural transport of carbon via rivers from the terrestrial biota to the oceans. The consequence of this transport is that net carbon uptake or loss for the ocean and biotic reservoirs differs from the net carbon fluxes between the atmosphere and the reservoirs. Sarmiento and Sundquist estimated the difference as about 0.6 Gt C y^{-1}.

The conversion between CO_2 fluxes and carbon fluxes is more complicated, as described by Enting and Mansbridge (1991). The estimated 0.86 Gt C y^{-1} CO_2 source from CO oxidation in the free atmosphere represents the balance of estimated sources of 0.3 Gt C y^{-1} from fossil carbon, 0.56 Gt C y^{-1} as CO from biotic sources, 0.05 Gt C y^{-1} as CH_4 from wetlands and 0.12 Gt C y^{-1} from other CH_4 sources, less a sink of 0.17 Gt C y^{-1} due to surface oxidation of CO.

Taking a 0.86 Gt C y^{-1} CO oxidation source of CO_2 corresponds to taking a fossil CO_2 source 0.3 Gt C y^{-1} lower than the fossil carbon source and a biotic CO_2 uptake flux that is 0.56 Gt C y^{-1} more negative than the biotic carbon uptake flux. The river carbon term will imply that the biotic carbon uptake flux would in turn be 0.6 Gt C y^{-1} more negative than the biotic carbon storage rate.

Conversely, to convert the CO_2 fluxes obtained from the inversion into estimates of carbon storage requires adding to the net CO_2 flux from the terrestrial biota 0.6 Gt C y^{-1} for river carbon and 0.56 Gt C y^{-1} for CO (or a modified value based on the estimated CO source).

3d Processes

Fossil carbon

The release of CO_2 from fossil carbon is characterised by the *fossil* space-time distribution described above. The source scaling factor for CO_2 is 1 by definition. We apply a factor of -1.41 for oxygen in our preliminary studies, based on the work of Keeling (1988), Keeling and Shertz (1992). The additional 0.41 reflects the uptake of oxygen during combustion of the hydrogen in hydrocarbon fuels. For $^{13}CO_2$ we use a $\delta^{13}C$ of $-27‰$ based on the data from Tans (1981) in the absence of more recent estimates. The question of incomplete combustion (releasing CO) needs to be addressed in connection with the distinctions between CO_2 fluxes and carbon fluxes, as discussed in Section 3c.

Air-sea flux

The standard cases of our air-sea flux assume no seasonal variation. As a consequence, we assume that no oxygen fluxes occur. The net CO_2 flux is the difference between two gross fluxes:

$$\Phi_{\mathrm{am}} = a\kappa p_{\mathrm{a}} \tag{10a}$$

and

$$\Phi_{\mathrm{ma}} = a\kappa p_{\mathrm{CO2}} \tag{10b}$$

where a is the area of the ocean region and κ is a gas-exchange coefficient. Thus the net flux is

$$S_{\mathrm{N}} = \Phi_{\mathrm{ma}} - \Phi_{\mathrm{am}} = a\kappa\Delta p_{\mathrm{CO2}} \tag{10c}$$

The determination of the net flux from direct measurements is limited by (a) uncertainties (of a factor of 2) in the gas-exchange coefficient and (b) the limited scope of the ocean p_{CO2} data set.

The $^{13}CO_2$ flux is given by

$$S^* = \alpha_{\mathrm{ma}} R_{\mathrm{m}} \Phi_{\mathrm{ma}} - \alpha_{\mathrm{am}} R_{\mathrm{a}} \Phi_{\mathrm{am}} \tag{11a}$$

The ocean contribution to the isotopic anomaly X is

$$\begin{aligned} S_X &= (S^*/R_{\mathrm{ref}} - S_{\mathrm{N}}) \times 1000 \\ &= [\alpha_{\mathrm{am}} R_{\mathrm{a}}/R_{\mathrm{ref}} - 1][\Phi_{\mathrm{ma}} - \Phi_{\mathrm{am}}] \times 1000 \\ &\quad + \Phi_{\mathrm{ma}}[\alpha_{\mathrm{ma}} R_{\mathrm{m}} - \alpha_{\mathrm{am}} R_{\mathrm{a}}] \times 1000/R_{\mathrm{ref}} \end{aligned} \tag{11b}$$

Thus the isotopic response splits into a component proportional to the net CO_2 flux, S_{N}, and a component proportional to the gross sea-to-air flux, Φ_{ma}. This second component is driven by the degree of isotopic disequilibrium $\alpha_{\mathrm{ma}} R_{\mathrm{m}} - \alpha_{\mathrm{am}} R_{\mathrm{a}}$ between the atmosphere and the mixed layer.

In dealing with the fractionation factors, we follow the approach of Heimann and Keeling (1989, Section 5) and only consider the effect of temperature on the equilibrium fractionation.

$$\alpha_{\mathrm{am}} = 0.9982 \tag{12a}$$

and

$$\alpha_{\mathrm{ma}} = \alpha_{\mathrm{am}}\alpha_{\mathrm{eq}} \tag{12b}$$

Heimann and Keeling (1989) used

$$\alpha_{\mathrm{eq}} = 1.02389 - \frac{9.483}{T + 273.15} \tag{12c}$$

The basis for such a parameterisation is that it is through the ratio or difference of α_{am} and α_{ma} that temperature has most influence on the isotopic fluxes and so it is reasonable to use the factor α_{eq} to parameterise this influence.

In summary, each ocean region is represented by two source components: a net flux term affecting both total CO_2 and the ^{13}C anomaly and a gross-flux term affecting only the ^{13}C anomaly. In each region, the same response distribution is used for the gross flux and net flux components.

For the net flux term the contribution to the isotopic anomaly involves the factor $[\alpha_{\mathrm{am}} R_{\mathrm{a}}/R_{\mathrm{ref}} - 1]$ which we obtain from the atmospheric $\delta^{13}C$ data and the fractionation factor given by (12*a*). The resulting response factors F_2 are listed in Table 1.

The disequilibrium contributions involve the product of gross flux and isotopic disequilibrium. For each region we have a product whose two factors can not be estimated independently. Formally, we fix the isotopic factor and adjust the gross flux; since the factors need to be discussed together, we defer the details until Section 3e.

Approaches such as that of Tans et al. (1990a) which estimate ocean fluxes need a 'conversion' term to give oceanic uptake. Similarly, the synthesis approach is estimating fluxes rather than storage; consequently the river carbon term must be added to determine net uptake. Our approach to the treatment of ^{13}C is consistent with this since, by using observed ocean ^{13}C data as the basis for calculating anomaly fluxes, we are using a 'flux' representation rather than an 'uptake' representation.

Biotic fluxes

The source of carbon due to the terrestrial biota is split into 3 components — a seasonal component, the 'land-use' component and the biotic uptake component. For each of these three components, we assume a $\delta^{13}C$ of $-25‰$. Again we follow the work of Keeling (1988), Keeling and Shertz (1992) in using a stoichiometric factor of 1.05 for relating carbon exchanges to oxygen exchanges between the atmosphere and biota. An extra contribution to the atmospheric $^{13}CO_2$ budget arises from an isotopic disequilibrium between the atmosphere and biota as described below.

Seasonal biotic exchange: The seasonal biotic component represents a steady-state biota where, over a full year, there is no net carbon flux to the atmosphere. The seasonal source is defined as the difference between the 'release' and 'uptake' distributions defined above, each having an amplitude of 45.6 Gt C y^{-1}.

Land-use change: In the analysis by Enting (1992) the deforestation term is essentially defined as the net carbon flux associated with changes of land-use. This is the quantity that was estimated by Houghton et al. (1983), Houghton (1993). The *land-use* space-time distribution is described above. The relative influences on CO_2, $^{13}CO_2$ and oxygen are as for the other biotic components.

Biotic uptake of CO_2: This term represents those biotic sinks of CO_2 that are not balanced by natural CO_2 sources at the point of uptake. Such uptakes occur when there is either storage of carbon in the ecosystem or a transport of carbon away from the system in a form other than atmospheric CO_2.

The storage term is generally equated to the effect of stimulated plant growth due to increased levels of atmospheric CO_2. However, if the 'land-use' term represents *all* the net CO_2 flux arising from change in land-use then, for a complete description, the 'uptake' term must include all other changes in terrestrial biomass. This will include both additional uptake from the effects of nutrient changes and reduced uptake resulting from toxification.

The contributions from carbon transported in forms other than atmospheric CO_2 are those that lead to the distinctions between CO_2 fluxes, carbon fluxes and carbon storage (see Section 3c). The first is the carbon that enters the atmosphere either as CO or as compounds that are oxidised to CO; the second is the component that is transported to the oceans via rivers.

We use the *uptake* distribution, i.e. the spatial distribution of NPP with the 'uptake' seasonal cycle. We run this term as a source for consistency with the sign convention of other components, even though CO_2-fertilisation and the imbalances arising from river transport and CO production represent sinks.

Isotopic disequilibrium of the terrestrial biota: The $\delta^{13}C$ of the terrestrial biota is changing due to the changing $\delta^{13}C$ of the atmospheric carbon taken up in photosynthesis. However this change will lag behind the atmospheric change and so the $\delta^{13}C$ of carbon released as CO_2 from the biota will be higher than that of carbon taken up. The disequilibrium term involves only the isotopic changes and does not appear in the total carbon budget. The effect of the isotopic disequilibrium will be proportional to the *gross* fluxes between the atmosphere and the terrestrial biota. For this component we use the *release* distribution, i.e. the spatial distribution of NPP with the 'release' seasonal cycle. (Appendix B describes a simple model used to quantify the isotopic disequilibrium effect.)

Carbon monoxide

The significance of atmospheric transport of CO was pointed out by Enting and Mansbridge (1991), following an analysis of the inversion problem by Enting and Newsam (1990). We take the $\delta^{13}C$ of the CO_2 produced as being characteristic of biotic and fossil carbon, on the basis that in a quasi-steady-state situation (i.e. time-scales longer than the CO lifetime of weeks to months), the isotopic compositions of sources and sinks of atmospheric CO must be the same. (The contribution of CH_4 to the CO oxidation source is very small.)

The issue of oxygen is more complex. The effect on the global oxygen budget will be given by the factor 1 (or 1.05) times the 0.471 factor converting from Gt C y^{-1} to ppmv y^{-1},

Region Units	Code	Latitudes Degrees	Area $10^{12}m^2$	κ $mol/m^2/yr/\mu atm$	S_E Gt C y^{-1}	$\delta_{eq} - \delta_a$ ‰
Atlant(B)	A	48N–90N	8.547	$*4.5 \times 10^{-2}$	−0.2	−0.94
Pacif(B)	B	48N–90N	7.816	$*4.5 \times 10^{-2}$	0.2	−1.08
Atlant(N)	C	16N–48N	23.829	3.0×10^{-2}	−0.3	0.67
Pacif(N)	D	16N–48N	40.508	3.0×10^{-2}	−0.3	0.32
Equatorial	E	16S–16N	108.328	2.2×10^{-2}	1.7	1.53
Atlant(S)	F	48S–16S	22.465	2.5×10^{-2}	−0.5	0.43
Pacif(S)	G	48S–16S	46.439	2.5×10^{-2}	−1.0	0.74
Indian(S)	H	48S–16S	31.870	2.5×10^{-2}	−0.7	0.46
Southern	I	90S–48S	51.624	$*6.0 \times 10^{-2}$	−0.2	−1.50

Table 2: Ocean regions used to define the spatial distributions of gross and net ocean flux terms. Code letters refer to Figure 2. Gas exchange coefficients, κ, e from Liss and Merlivat (1986): the *'s indicate large seasonal variations. Empirical fluxes, S_E, from Tans et al. (1990a) are about a factor of 2 larger than implied by the κ values.

since the CO oxidation is the end point of a 2-stage process of oxidising biotic (or fossil) carbon to give CO_2. When considering the spatial distributions, it is necessary to account for the fact that the 2 stages of oxidation can occur at different locations. Table 1 lists the factor $F_3(CO) = 0.5$ corresponding to the oxidation of CO for which our calculated response applies. The calculations in Section 6c use $F_3(CO) = 1.0$, treating the CO oxidation and production as producing oxygen at the same locations. A refined calculation would require a separate distribution for the effect of CO production on the oxygen distribution.

3e Prior estimates

Fossil: The value 5.606 Gt C y^{-1} is the average of 1986 and 1987 as reported in CDIAC (1991). The standard deviation of this prior estimate is taken as 5% of the total. Since the inversion is estimating CO_2 fluxes, we reduce the prior estimate to 5.3 Gt C y^{-1} to take account of CO emissions from incomplete combustion.

Net ocean flux: The estimation of air-sea fluxes from p_{CO2} data is subject to significant uncertainty, mainly due to uncertainties in the gas exchange coefficient — the κ of equations 10a—c. The difficulty is that 'empirical' estimates of the mean global exchange rate, based on uptake of ^{14}C (e.g. Broecker et al., 1980) differ by a factor of 2 from rates based on actual measurements of gas exchange (Liss and Merlivat, 1986). The 'empirical' estimates S_E in Table 2 are taken from Table 2 of Tans et al. (1990a) without correction for the changes in regional boundaries. The exception is that we have the northern Pacific split into 2 zones. On the basis of the p_{CO2} maps of Tans et al. (1990a), we suggest that, as a first approximation, the near-zero flux estimated by Tans et al. (1990a) represents a near-cancellation of two larger fluxes with the uptake comparable to that in the north Atlantic.

For the standard deviations of each ocean region we use a set of conservative estimates, generally ± 1 Gt C y^{-1}. The two smaller 'Boreal' regions are assigned ± 0.5 Gt C y^{-1}. The large equatorial region is assigned ± 1.5 Gt C y^{-1} and the southern

Pacific is assigned ± 1.5 Gt C y^{-1} on the grounds of limited p_{CO2} data.

The division of the isotopic flux into 'net flux' and 'gross flux' terms means that the 'net flux' contribution of the isotopic anomaly is fully specified as a multiple of the net carbon flux on the basis of the fractionation factor and the atmospheric $\delta^{13}C$ without the need to estimate any further parameters.

Gross ocean flux effect: This term affects only the isotopic distribution and arises from the isotopic disequilibrium between the atmosphere and the ocean. As implied by our terminology, these terms are proportional to the gross ocean-to-atmosphere CO_2 flux rather than the net flux. The gross flux term is expressed as

$$S_G = \Phi_{ma}[\alpha_{ma}R_m - \alpha_{am}R_a] \times 1000/R_{ref} = \Phi_{ma}\alpha_{am}\frac{R_a}{R_{ref}}\left[\alpha_{eq}\frac{R_m}{R_a} - 1\right] \times 1000 \quad (13)$$

Thus estimation of this term requires:

- The gross sea-to-air flux. This is subject to the same uncertainties regarding gas exchange coefficients as were described in connection with estimating net CO_2 fluxes from p_{CO2} differences;
- Data for the isotopic composition of ocean surface carbon;
- The temperature dependence of the fractionation factors.

Each of these factors involves significant uncertainties. However by formulating the isotopic flux so that all these uncertainties affect only one term, we are in a position to assess the consequences of these uncertainties. Since the various contributions to the disequilibrium effect can not be deduced independently from the atmospheric data, we take approximate values of the isotopic factors, regard these as fixed and incorporate any errors into the definition of an *effective* sea-to-air flux, $\Phi_{eff} \approx \Phi_{ma}\alpha_{am}R_a/R_{ref}$. Thus the estimation problem becomes one of estimating an unknown flux with a specified isotopic influence and no effect on the total carbon budget. However, the assignment of standard deviations to the prior estimates must take into account the uncertainties in each of the components contributing to the product.

As prior estimates of Φ_{eff} we use equation (10) in the form $a \times 300 \times 2\kappa_E$, with the κ_E values taken from Etcheto et al. (1991) as listed in Table 2 and with the factor of 2 included to make the fluxes comparable to the 'empirical' (^{14}C-based) flux estimates (Broecker et al, 1980). We take a 50% standard deviation as a relatively conservative estimate of the uncertainties in these estimates.

For the isotopic disequilibria, we use the data presented by Tans et al. (1993), converted to our grid using an area-weighted average. The values are listed in the final column of Table 2 and appear as the F_2 in Table 1 (with the G_2 obtained by multiplying the F_2 values by 0.471 ppmv/Gt C).

Seasonal biotic flux: For our standard case, we use a prior value of 1, since we have not normalised the response to a 1 Gt C y^{-1} source (since the net annual source is zero). The response is calculated (in ppmv) for our standard case with NPP of 45.6 Gt C y^{-1} and the seasonal variations of uptake and release as shown in Figure 3. We use an initial standard deviation of 0.5 to reflect the uncertainty in the NPP and in the relative timing of uptake and release.

Land-use change: The most detailed studies of the carbon flux due to land-use changes are those of Houghton et al. (1983, 1987), Houghton (1993). We follow the approach described by Enting (1992) taking an average of recent 'high' and 'low' estimates from Houghton (personal communication) and ascribing a range in proportion to that used in his earlier analyses, giving 2.2 ± 1.0 Gt C y^{-1}.

Biotic CO_2 uptake: As in the study by Enting (1992) our estimates for the biotic storage, which we attribute primarily to CO_2-enhanced growth, draw mainly on the study by Kohlmaier et al. (1987). We also note more recent work by Gifford (1993) and Polglase and Wang (1992). We use the range -1.6 ± 0.8 Gt C y^{-1} that was used by Enting (1992).

In addition to the extra carbon storage attributed to CO_2 fertilisation, this term has to include the 'unbalanced uptake' — the amount of CO_2 taken up that is not returned to the atmosphere as CO_2 but either enters the ocean via rivers or enters the atmosphere as CO. These terms contribute 1.2 Gt C y^{-1} — we take an overall prior estimate of the 'unbalanced' biotic CO_2 uptake as 2.8 ± 1.0 Gt C y^{-1}.

CO oxidation: The inversion only needs the net CO_2 production rate from CO oxidation. We use the value 0.86 Gt C y^{-1} (Enting and Mansbridge, 1991), rounded to the nearest 0.1 Gt C y^{-1} as for all other prior estimates. The standard deviation of 0.2 Gt C y^{-1} reflects the proportional uncertainty in the average OH concentration (and hence the CO sink) based on the study by Prinn et al. (1987).

Isotopic disequilibrium of the biota: The $\delta^{13}C$ of the terrestrial biota is changing due to the changing $\delta^{13}C$ of the atmospheric carbon taken up in photosynthesis. However this change will lag behind the atmospheric change and so the $\delta^{13}C$ of carbon released from the biota will be higher than that of carbon taken up. In their analysis, Quay et al. (1992) estimated this term as the gross flux times the $\delta^{13}C$ change over the residence time of biotic carbon. For short periods, the disequilibrium expression can be expressed as 'flux $\times$ residence time $\times$ rate of change of $\delta^{13}C$'. Quay et al. (1992) used 60 Gt C y^{-1} $\times$ 10 yr $\times 0.02‰ y^{-1} = 12‰$ Gt C y^{-1}. From the definition of the residence time, the effect of isotopic disequilibrium could be expressed as reservoir content $\times$ rate of change of $\delta^{13}C$ (with the rate of change taken as the average over the residence time). On this basis we use values rather higher than Quay et al., since the shorter-lived components will be reflecting a rate of change closer to $0.03‰ y^{-1}$ and the longer-lived components involve a reservoir that should include soil carbon and so be much larger than $60 \times 10 = 600$ Gt C.

In Appendix B, we use the biotic model of Emanuel et al. (1981) combined with the ice-core $\delta^{13}C$ data from Friedli et al. (1986) to estimate a biotic disequilibrium factor of $26.5‰$ Gt C y^{-1}.

As with the ocean isotope disequilibrium, the effect is a product of gross flux times isotopic disequilibrium, both of which are uncertain. Since we can not estimate the two factors separately, the estimation treats the problem in terms of a specified disequilibrium times an unknown gross flux. We use $0.3‰ \times 100 \pm 50$ Gt C y^{-1}.

4. Data sets

4a Time-averaging

The synthesis analysis presented in this report is intended to give estimates of the atmospheric carbon budget representative of the period 1986–1987. The mathematical procedure described in Section 2 assumes periodic sources leading to a concentration distribution in which a uniform global rate of increase is superimposed on a space-time distribution that has an annual periodicity. The results presented in Figure 4 show that the period around 1987 is one for which the assumption of a globally uniform increase appears justifiable.

The trend estimated for each site will reflect measurement errors, sampling inadequacies, small-scale source variations and longer-term globally coherent variations, most notably the ENSO signal. The influence of sampling problems, measurement errors and small-scale variations can be reduced by time-averaging. However, increasing the averaging time to reduce these errors will imply an averaging over more of the global-scale long-period variations and so the average becomes less representative of the chosen times.

These difficulties were addressed by Keeling et al. (1989b) in their synthesis analysis of atmospheric CO_2. They chose to look at the long-term averages, and ensured this by taking the global totals of reservoir fluxes from a box-diffusion model study that ignored the ENSO-scale variations. Consequently their atmospheric budgets that were nominally for particular years did not necessarily match the CO_2 growth rates for those years, but rather matched long-term growth rates around those years.

Our choices for averaging are somewhat arbitrary, but are based on a subjective assessment of the variability in the data. For seasonal cycles, we average over the entire length of the records. Apart from Mauna Loa, where the amplitude seems to have undergone a 'step' increase over the period 1975–1980 and remained high (e.g. Enting and Manning, 1989), there is little evidence of systematic long-term change in seasonal cycles of CO_2.

For the CO_2 trend we use a 4-year averaging as described in the next section. This seems to produce a set of estimates that are little affected by ENSO-scale variations. For the $\delta^{13}C$ trend we average over the available length of the CSIRO record (Francey et al., 1990), avoiding the last few years where a systematic change has become apparent. The spatial distribution of CO_2 shows considerable year-to-year variation whose nature is unclear. We have averaged over only 2 years — a compromise between error reduction and our desire to produce estimates representative of 1987.

4b CO_2

Our analysis of the atmospheric CO_2 cycle in terms of a quasi-steady-state means that there are three types of CO_2 data that are required:

- A globally representative rate of increase;
- A seasonal cycle for each site — this is assumed not to vary from year to year;
- The spatial distribution of de-seasonalised concentrations. We use the 1986–7 mean so that our reference time is Jan. 1 1987. Again we ignore interannual variability.

As well as needing estimates for these quantities, we also need a measure of the uncertainty of each estimate. Formally, the requirements are well-defined — we require a

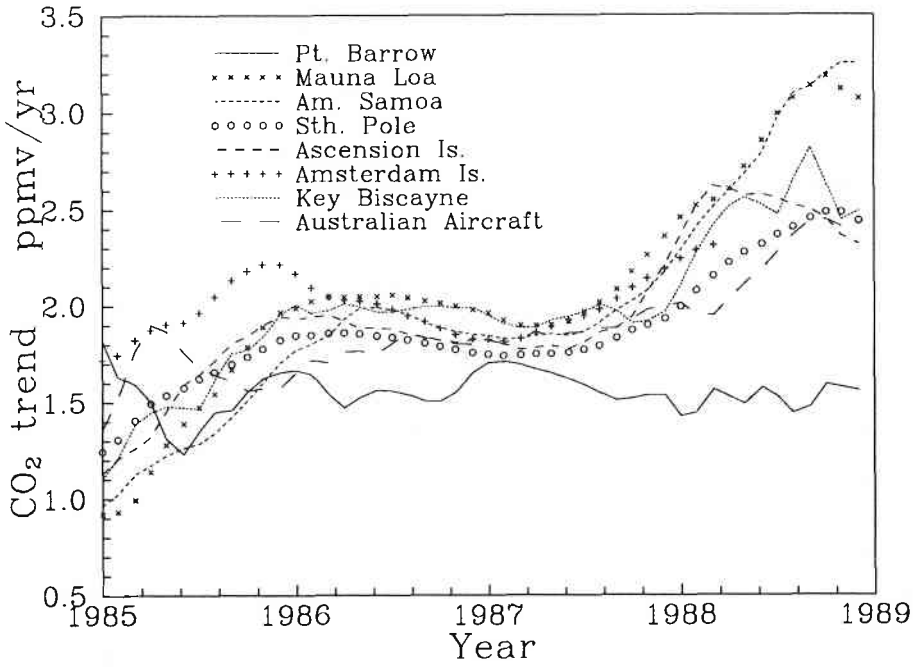

Figure 4: The rate of change of atmospheric CO_2 estimated from monthly flask data, using a 4-year smoothing period (CDIAC, 1991; Conway and Tans, 1990; Beardsmore, personal communication).

statistical model of each time series, formulated so that the estimation procedure can be analysed to produce the requisite error estimates. However, in spite of some preliminary work (e.g. Surendran and Mulholland, 1987), statistical modelling of CO_2 time series is a poorly explored area. Much statistical analysis of CO_2 data relies on regression analysis — the underlying statistical model: 'specified functions plus white noise' will often be too unrealistic to produce valid estimates of uncertainties. In the absence of detailed statistical modelling, we have adopted some *ad hoc* choices for the present study.

Our procedure for obtaining the trend term follows:

i. Perform a regression analysis to monthly mean data, fitting a quadratic function of time plus a fixed seasonal cycle.

ii. Subtract the seasonal cycle from the original series.

iii. For each time point at which the gradient is required, take a 4-year segment of the de-cycled series, centred on the time period of interest, and fit a straight line. The gradient of the line provides the estimate of the CO_2 trend.

Figure 4 shows the results of applying this procedure to the NOAA monthly mean flask data from Mauna Loa, the South Pole, Barrow, Samoa, Ascension Is., Amsterdam Is., Key Biscayne (as reported in CDIAC, 1991; see Conway and Tans, 1990 and references therein for further details) and CSIRO aircraft data (D. Beardsmore, personal communication).

Except for Barrow, these records show particularly coherent trends over the years 1986–7. We use the range 1.80 ± 0.15 ppmv y^{-1} on the basis of this figure. This may be a little too large to be truly representative of 1986–7, since there is some evidence that 1988 and 1989 had anomalously high CO_2 concentrations.

The seasonal cycles are obtained by a regression analysis of monthly mean concentrations for the various sites. The assumption of a fixed cycle means that the components can be estimated quite precisely since the full record is available for each fit. In this case we use the standard deviations as estimated by the regression analysis.

Since we are not analysing the seasonal cycle in detail, we have included only a single function describing the natural seasonal exchange with the biota. It is thus inappropriate to attempt to fit a large body of seasonal observations. (As discussed below, if we attempt to do so, the solution is severely distorted.) We therefore choose to fit only 1 site and use a mid-latitude northern hemisphere site as giving a representative reflection of the seasonal exchange component. Our 'standard' choice is to use the Azores data, for which we represent the seasonal cycle as

$$C_{\text{season}} = (1.443 \pm 0.182)\cos(2\pi t) + (4.146 \pm 0.182)\sin(2\pi t)$$
$$+(0.395 \pm 0.182)\cos(4\pi t) + (-1.535 \pm 0.182)\sin(4\pi t) \qquad \text{(Azores)}$$

Location	Code	Mean CO_2	Latitude	Longitude
Alert, Ellesmere Is.	ALT	348.75	82.50N	62.33W
Mould Bay, Canada	MBC	349.20	76.23N	119.33W
Barrow, Alaska	BRW	349.05	71.32N	156.60W
Ocean Station M	STM	348.00	66.00N	2.00E
Cold Bay, Alaska	CBA	348.90	55.20N	162.72W
Shemya Is., Alaska	SHM	349.45	52.75N	174.08E
Cape Meares, Oregon	CMO	349.30	45.00N	124.00W
Terceira Is., Azores	AZR	348.70	38.75N	27.08W
Sand Is., Midway Islands	MID	348.65	28.20N	177.38W
Key Biscayne, Florida	KEY	348.55	25.67N	80.17W
Cape Kumakahi, Hawaii	KUM	347.50	19.52N	154.82W
St. Croix, Virgin Is.	AVI	347.30	17.75N	64.85W
Guam Is,	GMI	348.40	13.43N	144.78E
Christmas Is.	CHR	347.40	2.00N	157.30W
Mahé Is., Seychelles	SEY	347.50	4.67S	55.17E
Ascension Is.	ASC	346.95	7.92S	14.42W
Cape Matatula, Samoa	SMO	346.25	14.25S	170.57W
Cape Grim, Tasmania	CGO	345.55	40.68S	144.73E
Palmer Station	PSA	345.85	64.92S	64.00W
South Pole	SPO	345.70	89.98S	24.80W

Table 3: CO_2 data — averages of 1986–1987 data from GMCC (1988). Each value is assigned a ± 0.3 ppmv uncertainty. In addition we use a global mean rate of change of 1.80 ± 0.15 ppmv y^{-1}.

The main CO_2 data set that we use is the mean concentrations from the NOAA flask sampling network. We use the average of the 1986 and 1987 annual means, as tabulated in

GMCC (1988). The values are listed in Table 3. The range of uncertainty is taken as 0.3 ppmv for each data point. This range is based on the work of Tans et al. (1990b) who used a simulation approach to explore the statistical characteristics of the NOAA flask sampling protocol. They simulated the statistical characteristics of the flask record by randomly sampling from the records of their continuous analyser records.

4c $^{13}CO_2$

The atmospheric $\delta^{13}C$ data come from the CSIRO global flask network. Air from the 'clean-air' sectors of the WMO baseline stations listed below is chemically dried on collection, and returned to the laboratory in 5 litre glass flasks at 100 kPa above ambient pressure. CO_2 is extracted cryogenically and analysed on a VG Micromass 602D mass spectrometer. The methods used in the selection, correction and conversion of these data to the international PDB scale are given in Francey and Goodman (1986, 1988). A summary of the early results is given in Francey et al. (1990). The annual averages in this paper have been obtained by first 'de-seasonalising' the data to minimise problems associated with uneven sampling (typically 1 sample per month, determined by conditions). The 'de-seasonalising' process consists of subtracting the seasonal cycle of the CO_2 record, multiplied by -0.05‰ppmv^{-1}. It should be pointed out that the inter-annual variability in the CSIRO data set over the 1982 to 1988 period is 3 to 5 times smaller than that reported by Keeling et al. (1989a). The reasons for this discrepancy have not yet been uncovered.

The values used in the inversions are averages over 1985--88, in ‰, Barrow: -7.899 ± 0.027; Mauna Loa -7.686 ± 0.017; Samoa: -7.638 ± 0.013; Cape Grim: -7.644 ± 0.010; South Pole -7.669 ± 0.010; with a global trend of -0.030 ± 0.005 ‰y^{-1}, based on our long $\delta^{13}C$ record from Cape Grim. The anomaly values, X, (in ‰ppmv) are Barrow: 35.25 ± 10.1; Mauna Loa: 109.08 ± 5.9; Samoa: 125.31 ± 4.5; Cape Grim: 123.01 ± 3.5; South Pole 114.4 ± 3.5; with a trend of -10.1 ± 1.7 ‰ppmv y^{-1}.

4d The rate of change of $\delta^{13}C$ of atmospheric CO_2

In the early stages of our study, it became apparent that the most important aspect of the $^{13}CO_2$ data for constraining the global budget was the global trend in atmospheric $\delta^{13}C$. In this section we analyse this trend, in conjunction with the CO_2 trend — in addition we re-analyse the studies of ^{13}C data by Quay et al. (1992) and Tans et al. (1993).

Table 4 gives the various estimates of contributions to the ^{13}C anomaly budget, expressed relative to a $\delta^{13}C$ of zero, i.e. following Tans (1980) and using $\delta^{13}C \times [C]$ as a conserved tracer. The atmospheric ^{13}C anomaly budget is:

$$\sigma_{\rm foss}\delta_{\rm foss} - (\Phi_{\rm am} - \Phi_{\rm ma})(\alpha_{\rm am}R_{\rm a}/R_{\rm standard} - 1) \times 1000$$

$$+\Phi_{\rm ma}\alpha_{\rm am}R_{\rm a}(\alpha_{\rm eq}R_{\rm m}/R_{\rm a} - 1) \times 1000 + (\sigma_{\rm def} + \sigma_{\rm fert})(\epsilon_{\rm b} + \delta_{\rm a})$$

$$+B_{\rm G}(\delta_{\rm b} - \epsilon_{\rm b} - \delta_{\rm a}) - \delta_{\rm a}\frac{d}{dt}N_{\rm a} - N_{\rm a}\frac{d}{dt}\delta_{\rm a} = 0 \qquad (14a)$$

For comparison the atmospheric budget for total carbon is written as

$$\sigma_{\rm foss} - (\Phi_{\rm am} - \Phi_{\rm ma}) + (\sigma_{\rm def} + \sigma_{\rm fert}) - \frac{d}{dt}N_{\rm a} = 0 \qquad (14b)$$

In principle, these two equations enable us to solve for any two unknown components of the atmospheric budget so long as all other components are known and as long as the two components have distinct isotopic signatures. Most interest has been in the case where the two components that are estimated are the net air-sea flux $S_N = \Phi_{am} - \Phi_{ma}$ and the net biotic flux $B_N = \sigma_{def} + \sigma_{fert}$.

The equation for total carbon balance (14b) is generally interpreted as an equation for net carbon storage/loss, but it can equally well be regarded as an equation representing net fluxes — as discussed above, the transport of carbon via rivers implies a distinction between net fluxes and net storage. We use B_N^+ and S_N^+ to denote net biotic carbon loss and net ocean carbon storage. (In considering global budgets, the distinction between CO_2 fluxes and carbon fluxes disappears since essentially all CO is oxidised to CO_2.) In these terms the total carbon balance is

$$B_N - S_N + \sigma_{foss} - \frac{d}{dt}N_a = 0 \qquad \text{(carbon flux)} \tag{15a}$$

or

$$B_N^+ - S_N^+ + \sigma_{foss} - \frac{d}{dt}N_a = 0 \qquad \text{(carbon storage)} \tag{15b}$$

The 'flux' form of the $^{13}CO_2$ balance follows directly from equation (14a) as:

$$\sigma_{foss}\delta_{foss} - S_N(\epsilon_{am} + \delta_a) + \Phi_{ma}(\delta_{eq} - \delta_a) + B_N(\epsilon_b + \delta_a)$$

$$+B_G(\delta_b - \epsilon_b - \delta_a) - \delta_a\frac{d}{dt}N_a - N_a\frac{d}{dt}\delta_a = 0 \tag{16a}$$

Given the distinctions described above, we can now calculate the various terms in the balance as presented in Table 4.

- For 1987 the rate of change of atmospheric CO_2 is 1.8 ppmv y^{-1} (3.8 Gt C y^{-1}) and the $\delta^{13}C$ is $-7.8‰$. For the period 1970–90, Quay et al. (1992) use 2.9 Gt C y^{-1} and $-7.56‰$.

- For 1987 we use N_a = 739 Gt C (348 ppmv) and $\frac{d}{dt}\delta_a = -0.03‰ y^{-1}$. For 1970–1990 Quay et al. use 717 Gt C and $-0.02‰ y^{-1}$.

- The fossil $\delta^{13}C$ is taken as $-27.2‰$, with sources of 5.606 Gt C y^{-1} for 1987 and 5.1 Gt C y^{-1} for 1970–90.

- Quay et al. use a biotic disequilibrium term of $12‰$Gt C y^{-1}. For the basis of comparison, Tans et al. (1993) use the same value. As discussed above, we believe a larger value is appropriate. We use $30‰$Gt C y^{-1} rounded from the value calculated in Appendix B.

- The isotopic effect of the net air-sea flux is $S_N(\epsilon_{am} + \delta_a) = 9.6S_N$.

- The effect of isotopic disequilibrium between the atmosphere and ocean is taken as $0.43‰ \times 85$ Gt C y^{-1} by Tans et al. (1993). As discussed above, the difficulty in determining this term comes from the fact that it involves a weighted average over both positive and negative values of air-sea disequilibrium, with some uncertainty in both the $\delta^{13}C$ and the weighting factors.

- An alternative analysis of ocean ^{13}C in terms of uptake (i.e. storage) rather than fluxes was given by Quay et al. (1992).

The new feature introduced by Quay et al. (1992) was the use of the temporal change in depth-integrated ocean $\delta^{13}C$ to obtain terms related to the ocean carbon uptake. They used the 'storage' form of the atmospheric $^{13}CO_2$ budget:

$$\sigma_{\rm foss}\delta_{\rm foss} - a\frac{d}{dt}\int \delta_{\rm m}(z)C(z)\,dz + B_{\rm N}^{+}(\epsilon_{\rm b}+\delta_{\rm a})$$

$$+B_{\rm G}(\delta_{\rm b}-\epsilon_{\rm b}-\delta_{\rm a}) - \delta_{\rm a}\frac{d}{dt}N_{\rm a} - N_{\rm a}\frac{d}{dt}\delta_{\rm a} = 0 \qquad (16b)$$

The ocean ^{13}C change was expressed as:

$$a\frac{d}{dt}\int_0^z C(z)\delta_{\rm m}(z')\,dz' = a\bar{C}\frac{d}{dt}\int_0^z \delta_{\rm m}(z')\,dz' + a\bar{\delta}_{\rm m}\frac{d}{dt}\int_0^z C(z')\,dz'$$

$$= a\bar{C}\frac{d}{dt}\int_0^z \delta_{\rm m}(z')\,dz' + \bar{\delta}_{\rm m}S_{\rm N}^{+} \qquad (17a)$$

Quay et al. (1992) used:

- A mean ocean $\delta^{13}C$ of $\delta_{\rm m} = 1.7‰$;
- A mean ocean carbon content of $\bar{C} = 2.0$ mol m^{-3} (24 g m^{-3});
- An ocean area of $a = 360 \times 10^{12}$ m^2;
- A change in depth-integrated $\delta^{13}C$ of $-208‰$m over 20 years, i.e. an average rate of change of $-10.4‰$m y^{-1}.

so that the ocean ^{13}C anomaly storage term is (in $‰$Gt C y^{-1})

$$a\frac{d}{dt}\int_0^z C(z)\delta_{\rm m}(z')\,dz' = -89.9 + 1.7S_{\rm N}^{+} \qquad (17b)$$

The values in Table 4 provide the basis for determining $B_{\rm N}$ and $S_{\rm N}$ (or $B_{\rm N}^{+}$ and $S_{\rm N}^{+}$). The total anomaly, which has to sum to zero, will depend (weakly in the case of the Quay et al. analysis) on $S_{\rm N}$ and $B_{\rm N}$. The constraint from the total carbon budget is that $B_{\rm N} - S_{\rm N} = B_{\rm N}^{+} - S_{\rm N}^{+} = \dot{N}_{\rm a} - \sigma_{\rm foss}$. The solutions defined by the two constraints are shown in the last two lines of the table.

Table 4 illustrates the discrepancy between the approaches of Quay et al. (1992) giving $B_{\rm N}^{+} = -0.2$ ($B_{\rm N} \approx -0.8$) and Tans et al. (1993) giving $B_{\rm N} = -1.8$ ($B_{\rm N}^{+} \approx -1.2$). The discrepancy is about 1.0 Gt C y^{-1} after including the conversion between fluxes and reservoir storage (approximately 0.6 Gt C y^{-1} due to transport of carbon through rivers).

The process of using the combination of isotopic data with constraints on total carbon can be represented graphically as shown in Figure 5. Each component is represented as a vector. The vertical component of each vector represents the carbon flux, the horizontal component represents the isotopic anomaly flux. Thus the effective $\delta^{13}C$ of the fluxes is represented by the angle of the vector. Figure 5 is plotted using anomalies relative to a $\delta^{13}C$ of 0. A change of reference ratio would correspond to a horizontal shearing of the plot (an affine transformation) but would not change the relations between the vectors. (This type of diagram is a two-component generalisation of the carbon budget diagrams introduced by Enting, 1993.)

Process Period	Expression	Quay 1970–90	Tans 1970–90	This report 1987
ATMOS.				
$\frac{d}{dt}CO_2$	$-\delta_a \frac{d}{dt} N_a$	21.9	23.1	29.8
$\frac{d}{dt}\delta^{13}C$	$-N_a \frac{d}{dt}\delta_a$	14.3	14.3	22.2
FOSSIL				
Fossil	$\sigma_{foss}\delta_{foss}$	−138.7	−136.0	−152.5
BIOTA				
Net		$-25B_N^+$	$-26.6B_N$	$-25B_N$
Diseq.	$B_G(\delta_b - \epsilon_b - \delta_a)$	12.0	12.0	26.5
OCEAN				
Diseq.	$\Phi_{ma}(\delta_{eq} - \delta_a)$	—	36.6	36.6
Net flux	$-S_N(\epsilon_{am} + \delta_a)$	—	$9.6S_N$	$9.6S_N$
Total	$a\frac{d}{dt}\int \delta_m(z)C(z)dz$	$89.9 - 1.7S_N^+$	—	—
Total anomaly	$= 0$	$-0.6 - 1.7S_N^+$ $-25B_N^+$	$-50 + 9.6S_N$ $-26.6B_N$	$-38.1 + 9.6S_N$ $-25B_N$
$B_N - S_N$	$= \dot{N}_a - \sigma_{foss}$	—	−2.0	−1.8
$B_N^+ - S_N^+$	$= \dot{N}_a - \sigma_{foss}$	−2.2	—	—
Ocean Biotic		$S_N^+ = 2.0$ $B_N^+ = -0.2$	$S_N = 0.2$ $B_N = -1.8$	$S_N = 0.4$ $B_N = -1.4$

Table 4: Comparison of alternative interpretations (Quay et al., 1992; Tans et al., 1993 and the present study) of the atmospheric $^{13}CO_2$ budget, expressed as anomalies relative to a reference $\delta^{13}C$ of 0. Units are ‰Gt C y^{-1} except for the last four rows which give (in Gt C y^{-1}) the two forms of extra constraints from the total carbon budget and the solutions obtained by combining the appropriate carbon budget constraint with the requirement that the total $^{13}CO_2$ anomaly is zero.

Figure 5 is plotted using a biotic disequilibrium of 30‰Gt C y^{-1} rounded from the estimate 26.5‰Gt C y^{-1} used in Table 4. The solutions are obtained by equating the oceanic uptake to the sum of non-oceanic 'inputs'. The sum is taken as including a biotic release or uptake whose magnitude is unknown. The 'inventory' solution is where the inventory constraint describing oceanic carbon and $^{13}CO_2$ increase crosses the biotic release line. The 'flux' solution is found from the point where the ocean contribution, expressed as disequilibrium plus net flux at −9.6‰, crosses the biotic uptake line. In each case, the use of a biotic disequilibrium of 30‰Gt C y^{-1} rather than 12‰Gt C y^{-1} has led to a larger estimate of oceanic uptake than in the original analyses but has not greatly reduced the discrepancy. (Note that a difference of about 0.6 Gt C y^{-1} between the 'flux' and 'inventory' solutions is expected because of the distinction between flux and storage.)

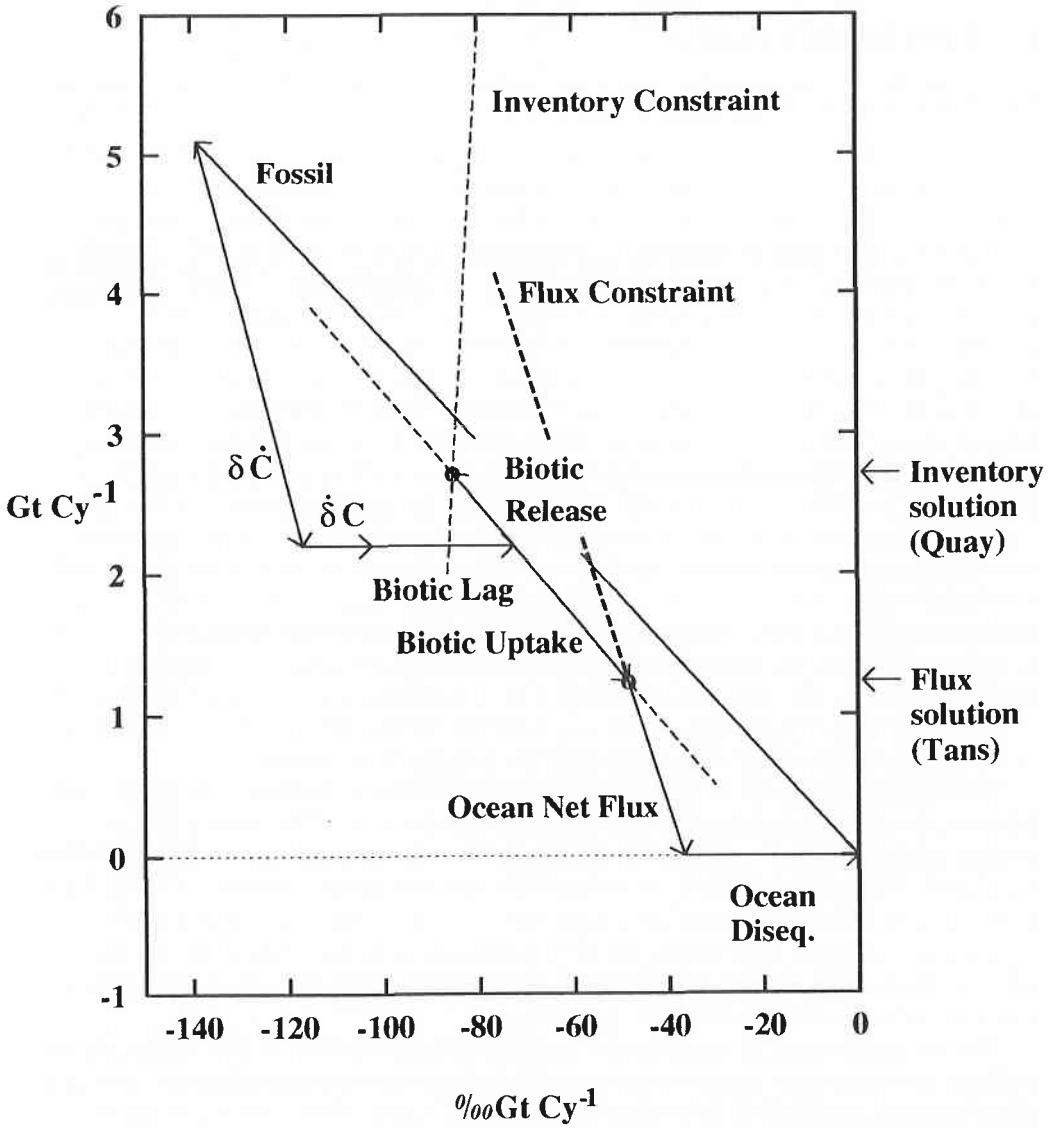

Figure 5: Vector representation of the atmospheric budgets for $^{13}CO_2$ and total carbon. Each vector represents a source component with the gradient indicating the $\delta^{13}C$ of the flux. The $^{13}CO_2$ and CO_2 budgets are expressed as fossil flux − atmospheric change + isotopic lag of biota ± net biotic term = net ocean uptake. The circles show the solutions with oceanic uptake defined by the ^{13}C inventory ('Quay' solution) and the $^{13}CO_2$ flux ('Tans' solution).

5. Synthesis results

5a Inversion of CO_2 distributions

Table 5 gives the estimates of the components of the atmospheric carbon budget, derived by applying the synthesis analysis to the data sets described in Section 4. An important feature of the table is the extent to which each level of analysis contributes to reducing the uncertainties. (The isotopic disequilibrium components were included in each calculation but are not tabulated, since they do not contribute to the carbon budget.) Firstly, we list the prior estimates of the various sources. Secondly, we give the least-squares estimate using only the priors and the global CO_2 trend. It will be seen that only small changes are required from the priors in order to achieve a balanced budget. Thirdly, we include the $\delta^{13}C$ trend as well as the CO_2 trend. This analysis is comparable to that shown in the last column of Table 4, except that we are allowing for the uncertainties in each of the components, both in the trend data that we fit and in the disequilibrium contributions which we adjust to help fit the data. Fourthly, we include the CO_2 data from the global network. At this stage, significant reductions in the range of uncertainty are obtained for many of the components. The final column gives estimates based on the CO_2 concentration data (trend plus spatial distribution) without the use of the $\delta^{13}C$ trend. We can compare the importance of the spatial distribution of CO_2 relative to the $\delta^{13}C$ trend by comparing the uncertainties. It can be seen that while the inversion of the spatial distribution greatly reduces the uncertainties in the regional fluxes, this improved knowledge does not translate into a comparable reduction of uncertainty in the global total. At the levels of data uncertainty used here, a knowledge of the $\delta^{13}C$ trend gives the better estimate of the global net air-sea flux.

The solutions presented in Table 5 suffer from considerable instability. In many cases the changes are large compared to the estimated uncertainties. This implies that the estimated uncertainties are probably underestimates — i.e. that the statistical analysis is inadequate. The problem appears to be that there are two distinct solutions. The spatial distribution of CO_2 appears to imply a large oceanic sink — this is a similar result to that obtained by Keeling et al. (1989b). The $\delta^{13}C$ trend (interpreted in terms of air-sea fluxes) seems to imply a small ocean sink. The least-squares approach gives a set of 'compromise' estimates without really resolving the problem.

One noticeable point of the fit to the spatial distribution of CO_2 is that several of the residuals are larger than seems probable under the assumption of normal errors with 0.3 ppmv standard deviation. In order to explore the significance of this, we repeat the fits to the spatial data with the CO_2 data from KUM, CMO and AZR effectively excluded by the process of assigning large uncertainties. The results of the fits are tabulated in Table 6. Comparing Tables 5 and 6, and in particular the North Atlantic sink, it will be seen that, as expected in a least squares fit, data with large residuals have a very great influence on the solution when they are included.

5b $^{13}CO_2$ gradient constraints

Before discussing the fit to the spatial distribution of $\delta^{13}C$, we consider the latitudinal gradient of $\delta^{13}C$ resulting from the sources estimated in Table 6. Figure 6 shows 4 cases together with data from the CSIRO sampling program. Each model result is calculated with the CO_2 outliers excluded. The dotted curve (the 'CO_2 only' column of Table 6) uses only CO_2 data. The curve with the short dashes uses CO_2 data and the $\delta^{13}C$ trend (the

Process	Prior	$\frac{d}{dt}CO_2$	Trends	Trends&CO_2	CO_2 only
Fossil	5.3 ± 0.3	5.30 ± 0.30	5.24 ± 0.30	5.18 ± 0.29	5.21 ± 0.30
Land-use	2.2 ± 1.0	2.16 ± 0.96	1.63 ± 0.88	1.43 ± 0.85	1.89 ± 0.93
Bio. uptake	-2.8 ± 1.0	-2.84 ± 0.96	-3.36 ± 0.88	-3.14 ± 0.81	-2.77 ± 0.87
CO oxid.	0.9 ± 0.2	0.90 ± 0.20	0.88 ± 0.20	0.88 ± 0.20	0.90 ± 0.20
Seasnl. bio.	1.0 ± 0.5	1.00 ± 0.50	1.00 ± 0.50	0.71 ± 0.04	0.72 ± 0.04
n:Atlant(B)	-0.2 ± 0.5	-0.21 ± 0.49	-0.18 ± 0.49	-0.78 ± 0.26	-0.84 ± 0.27
n:Pacif(B)	0.2 ± 0.5	0.19 ± 0.49	0.22 ± 0.49	0.54 ± 0.19	0.50 ± 0.19
n:Atlant(N)	-0.3 ± 1.0	-0.34 ± 0.96	-0.23 ± 0.95	-0.55 ± 0.36	-0.66 ± 0.37
n:Pacif(N)	-0.3 ± 1.0	-0.34 ± 0.96	-0.23 ± 0.95	-0.19 ± 0.43	-0.31 ± 0.44
n:Equat.	1.7 ± 1.5	1.61 ± 1.36	1.86 ± 1.34	2.22 ± 0.82	1.88 ± 0.86
n:Atlant(S)	-0.5 ± 1.0	-0.54 ± 0.96	-0.43 ± 0.95	-0.50 ± 0.81	-0.57 ± 0.81
n:Pacif(S)	-1.0 ± 1.5	-1.09 ± 1.35	-0.84 ± 1.34	-1.76 ± 1.01	-1.85 ± 1.02
n:Indian(S)	-0.7 ± 1.0	-0.74 ± 0.96	-0.63 ± 0.95	-0.19 ± 0.74	-0.23 ± 0.74
n:Southern	-0.2 ± 1.0	-0.24 ± 0.96	-0.13 ± 0.95	0.65 ± 0.45	0.66 ± 0.45
Σ Ocean	-1.3 ± 3.2	-1.69 ± 1.35	-0.58 ± 1.09	-0.56 ± 1.02	-1.42 ± 1.23

Table 5: Estimates of strengths of source components derived using the Bayesian synthesis technique with the standard priors from Table 1. The headings of columns 2 to 5 indicate the data from which the estimates are obtained. Regional suffices for oceans refer to far north (B for boreal), north (N) and south (S). Prefix 'n:' refers to the contributions of net air-sea flux. Note that these estimates refer to CO_2 fluxes rather than either carbon fluxes or carbon storage.

Process	Prior	Trends&CO_2	CO_2 only
Fossil	5.3 ± 0.3	5.21 ± 0.29	5.26 ± 0.29
Land-use	2.2 ± 1.0	1.60 ± 0.86	2.15 ± 0.93
Bio uptake	-2.8 ± 1.0	-2.95 ± 0.82	-2.48 ± 0.88
CO oxid.	0.9 ± 0.2	0.89 ± 0.20	0.91 ± 0.20
Seasnl. bio.	1.0 ± 0.5	0.73 ± 0.04	0.74 ± 0.04
n:Atlant(B)	-0.2 ± 0.5	-0.76 ± 0.26	-0.84 ± 0.27
n:Pacif(B)	0.2 ± 0.5	0.42 ± 0.20	0.37 ± 0.21
n:Atlant(N)	-0.3 ± 1.0	-1.43 ± 0.41	-1.59 ± 0.43
n:Pacif(N)	-0.3 ± 1.0	0.26 ± 0.54	0.11 ± 0.55
n:Equat.	1.7 ± 1.5	2.52 ± 0.84	2.11 ± 0.87
n:Atlant(S)	-0.5 ± 1.0	-0.53 ± 0.81	-0.62 ± 0.81
n:Pacif(S)	-1.0 ± 1.5	-1.83 ± 1.01	-1.94 ± 1.02
n:Indian(S)	-0.7 ± 1.0	-0.27 ± 0.74	-0.32 ± 0.74
n:Southern	-0.2 ± 1.0	0.66 ± 0.45	0.67 ± 0.45
Σ Ocean	-1.3 ± 3.2	-0.96 ± 1.03	-2.05 ± 1.24

Table 6: Estimates of strengths of source components derived as for Table 5 except that the CO_2 data for KUM, AZR and CMO has been effectively ignored by assigning large uncertainties.

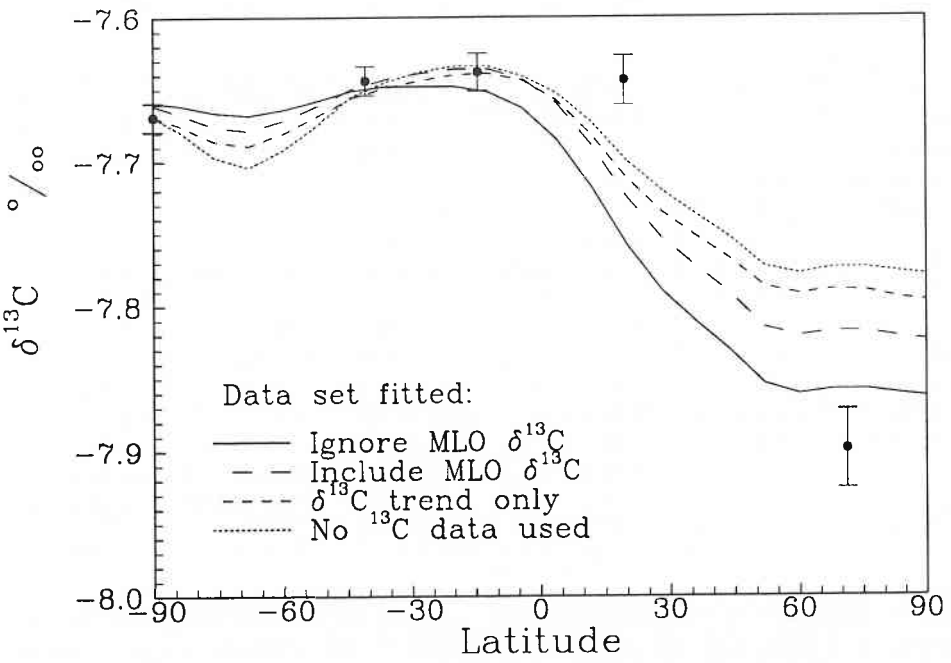

Figure 6: Zonally-averaged $\delta^{13}C$ corresponding to the source estimates from Tables 6 and 7. All the estimates use the spatial distribution and trend of CO_2. The dotted curve uses no other data, the short dashes add only the $\delta^{13}C$ trend to the data fitted, the long dashes include all 5 sites from the CSIRO network (as well as using the trend), the solid curve excludes Mauna Loa from the fit. The data from the CSIRO network are also shown with the uncertainty ranges used in the inversion.

'Trends & CO_2' column of Table 6). Clearly the model predicts too small a gradient in the northern hemisphere. The calculated values are too low for Mauna Loa and too high for Barrow.

The comparison is complicated by 2 factors. Firstly, Mauna Loa is not a surface site. It is unclear whether there should be a significant vertical gradient in $\delta^{13}C$ — the data presented by Keeling et al. (1989a, Table 6) show a significant interannual variation in the difference between Cape Kumakahi and Mauna Loa. 1986, the first year of our nominal analysis period, was one for which the $\delta^{13}C$ observations showed one of the largest differences between Mauna Loa and Cape Kumakahi (0.04‰). Adjusting the Mauna Loa data by −0.04‰ would improve the fit to the model.

Secondly, the discrepancy is even greater for Barrow than is suggested by the figure since the model exhibits considerable longitudinal variation at high northern latitudes and the model calculation for Barrow lies well above the zonal mean. The longitudinal variation arises from a covariance between the seasonal biotic source and seasonal variations in transport. Apparently the main effect is the seasonal variation in convection. In winter, more stable conditions over the Eurasian sector retain air with high CO_2 and low $\delta^{13}C$ near the surface so that sites in the American sector have CO_2 below the zonal mean and $\delta^{13}C$

Process	Prior	All	Ex δ	Ex CO_2	Ex δ, CO_2
Fossil	5.3 ± 0.3	5.26 ± 0.29	5.35 ± 0.29	5.29 ± 0.29	5.39 ± 0.29
Land-use	2.2 ± 1.0	0.90 ± 0.84	0.99 ± 0.84	1.05 ± 0.84	1.14 ± 0.84
Bio uptake	-2.8 ± 1.0	-2.56 ± 0.78	-2.35 ± 0.78	-2.39 ± 0.78	-2.18 ± 0.78
CO oxid.	0.9 ± 0.2	0.87 ± 0.20	0.88 ± 0.20	0.87 ± 0.20	0.88 ± 0.20
Seasnl. bio.	1.00 ± 0.5	0.72 ± 0.04	0.73 ± 0.04	0.74 ± 0.04	0.75 ± 0.04
n:Atlant(B)	-0.2 ± 0.5	-0.86 ± 0.26	-0.91 ± 0.26	-0.87 ± 0.26	-0.88 ± 0.26
n:Pacif(B)	0.2 ± 0.5	0.51 ± 0.19	0.47 ± 0.19	0.40 ± 0.20	0.36 ± 0.20
n:Atlant(N)	-0.3 ± 1.0	-0.59 ± 0.35	-0.66 ± 0.35	-1.47 ± 0.41	-1.56 ± 0.41
n:Pacif(N)	-0.3 ± 1.0	0.30 ± 0.42	0.32 ± 0.42	0.13 ± 0.53	0.13 ± 0.53
n:Equat.	1.7 ± 1.5	2.32 ± 0.81	2.19 ± 0.81	2.65 ± 0.83	2.52 ± 0.83
n:Atlant(S)	-0.5 ± 1.0	-0.48 ± 0.81	-0.48 ± 0.81	-0.51 ± 0.81	-0.51 ± 0.81
n:Pacif(S)	-1.0 ± 1.5	-1.72 ± 1.01	-1.82 ± 1.01	-1.78 ± 1.01	-1.88 ± 1.01
n:Indian(S)	-0.7 ± 1.0	-0.22 ± 0.74	-0.22 ± 0.74	-0.29 ± 0.74	-0.30 ± 0.74
n:Southern	-0.2 ± 1.0	0.66 ± 0.45	0.69 ± 0.45	0.66 ± 0.45	0.69 ± 0.45
Σ Ocean	-1.3 ± 3.2	-0.68 ± 0.95	-1.07 ± 0.96	-1.03 ± 0.96	-1.43 ± 0.97

Table 7: Estimates of CO_2 fluxes derived using the Bayesian synthesis technique with the standard priors from Table 1 for the CO_2 fluxes and fitting the spatial distribution of $\delta^{13}C$. The 'All' column uses the spatial distributions and trends of CO_2 and $\delta^{13}C$. The exclusions in the other columns are CO_2: the outliers KUM, CMO and AZR; and δ: the Mauna Loa $\delta^{13}C$.

above the zonal mean. While this mechanism is qualitatively reasonable, it is harder to check quantitatively. A similar systematic variation is not found when the model described by Law et al. (1992) is used with our seasonal sources (R. Law, personal communication).

The difficulty in fitting the northern hemisphere $\delta^{13}C$ gradient has been a persistent problem. Pearman and Hyson (1986) produced a similarly small gradient, although at that time there were insufficient data to indicate a problem. Keeling et al. (1989b) found similar difficulties as have recent 2-D model studies by Tans (personal communication).

Our attempts to fit the $\delta^{13}C$ gradient have brought out further instability in the analysis — as before this presumably reflects the attempt to fit inconsistent information. The curve with long dashes in Figure 5 is the 'Ex CO_2' column of Table 7 where we fit all the $^{13}CO_2$ data but exclude the CO_2 outliers.

Table 7 lists the estimates that are obtained for the carbon budget when we include the spatial distribution of $\delta^{13}C$. The cases cover fits with and without the 'outlier' CO_2 data and with and without the Mauna Loa $\delta^{13}C$ data — so that all 4 combinations are shown. The reason for considering fits that exclude the $\delta^{13}C$ for Mauna Loa, is that our fits are only for surface concentrations.

The solid curve in Figure 5 shows the zonal mean $\delta^{13}C$ from the final column of Table 7, i.e. the case in which the Mauna Loa $\delta^{13}C$ and the 'outlier' CO_2 data are excluded. The fit is clearly improved and we take this case as our 'preferred' solution. Equally clearly, a better fit would be desirable. The Barrow data are still below the zonal mean, even though the model has the Barrow grid cell higher than the zonal mean. Similarly, Mauna Loa lies above the zonal mean by an amount that exceeds the largest annual mean vertical differences (KUM vs. MLO) measured by Keeling et al. (1989a).

6. Extensions

The results presented in the previous section suggest a number of possible extensions to the calculations that lie beyond the scope of this report.

6a Disaggregating biotic fluxes

The assumption underlying the synthesis approach is that the space-time distribution of each of the source components is known apart from an overall 'source-strength' factor. There is however the risk that this assumption can 'overspecify' the problem. As an example, our first calculations with the present algorithm used a more comprehensive set of seasonal data. The resulting estimates for mean source components were extremely unrealistic — since the single seasonal source component used in the inversion did not have the flexibility to completely explain the observations, the data were fitted with combinations of time-invariant sources whose seasonal response happened to fit the 'unexplained' part of the observed seasonal variation.

For ocean inverse problems, Wunsch and Minster (1982) recommend that for a realistic treatment of uncertainties, an underdetermined formulation of the problem is required. The principle is that in an ill-conditioned problem the data will specify only a small number of degrees of freedom in the solution but that the problem should be formulated so that the resolution is determined *by the data* and not by some arbitrary initial prescription of a restricted solution space.

In this section we consider possible disaggregations of the biotic source/sink contributions. The consideration of explicit 'noise' contributions representing departures from the assumed space-time distributions is the topic of Section 6b.

The most obvious form of disaggregation is in terms of spatial components. The biotic data set that we used suggests the decomposition of the *uptake* and *release* distributions into 8 distinct components each, corresponding to (i) Tropical forest — America; (ii) Tropical forest — Africa; (iii) Tropical forest — Asia; (iv) Temperate evergreen; (v) Temperate deciduous; (vi) Boreal forest; (vii) Grassland; (viii) Other.

For land-use change, a natural decomposition is into 4 distinct components corresponding to: (i) Tropical forest — America; (ii) Tropical forest — Africa; (iii) Tropical forest — Asia; (iv) Temperate and boreal forests.

However an alternative to the spatial decompositions would be a further decomposition on the basis of processes. Some possibilities are:

i. The uptake term could be broken down on a process basis, firstly separating the CO terms and the 'river flux' terms from the net carbon storage component and then separating the 'fertilisation' component from other effects such as toxification.

ii. The 'land-use' term could be broken down on a process basis, separating the effects of biomass burning, release of soil carbon, regrowth etc.

iii. It may also be relevant to consider a spatial disaggregation of the terms describing isotopic disequilibrium of the biota if more $\delta^{13}C$ data becomes available.

iv. Disaggregation of the seasonal biotic source. This could improve the fit and also exploit data on seasonal variations of $^{13}CO_2$.

The exploration of these various disaggregations is beyond the scope of this report.

6b Extended error analysis

In their discussion of CO_2 observations, Enting and Pearman (1993) described the various contributions to the observed variability. They noted any variability that can not be treated within a model has to be regarded as 'noise' and that much of such 'noise' represents actual sources that are neglected.

This consideration is particularly relevant to synthesis studies since the basis of the synthesis is that the space-time variation of the various source components is known apart from a single scale factor. Any variations from this assumption are generally neglected. As noted above, Wunsch and Minster (1982) suggest that such overspecification of the solution can lead to unrealistic results. In particular, error estimates are likely to be too small.

Formally, the uncertainties in the spatial (and/or temporal) distributions can be dealt with by further disaggregation. However this can lead to a significant increase in computational complexity. In addition, it may be inappropriate to assume independent prior uncertainties for components in a finely divided source region.

We have performed some preliminary calculations exploring the possibility of using alternative representations of source variability. We consider an expansion of the source distribution in terms of spatial moments, in analogy with the multipole expansion in electrostatics. The approximation that we consider is to represent a source as a 'total' with a specified spatial distribution with the 'correction' being the 'dipole moment'. This dipole source has zero net flux since it consists of a matched source and sink. Such a 'dipole' will influence atmospheric concentrations by an amount proportional to the product of the source/sink strength and the distance between them. Strictly, this will be true only on average and only in the limit as the spacing goes to zero. However we have performed numerical tests with spacings of 8° and 24° of latitude and found sufficient agreement to suggest that the dipole approximation will be a useful way of characterising source uncertainty. (We have also confirmed that the greatest influence comes for the north-south component of the dipole moment vector, as would be expected on the basis of more rapid longitudinal mixing).

In a Bayesian formulation, the 'total' would be the best estimate of the source so that the prior expectation of the dipole component would be zero. Its standard deviation would be the root-mean-square dipole moment. In cases where the statistics of the source distribution can be characterised by a random field, the mean-square dipole moment is proportional to the second spatial moment of the autocorrelation.

The dipole approach has the potential for reducing the computations and also allowing the incorporation of more complex statistical characterisations of the prior source estimates. Further investigations of the approach are currently in progress and will be reported elsewhere.

6c The role of oxygen data

The response factors listed in Table 1 include factors describing the influence of the various source components on atmospheric oxygen. It has recently become possible to measure atmospheric oxygen with a precision that is, in principle, sufficient to provide useful constraints on the atmospheric carbon budget (Keeling, 1988; Keeling and Shertz, 1992). In practice, we encounter a difficulty similar to that involved in the interpretation of the isotopic data: additional effects occur, involving additional quantities to be estimated.

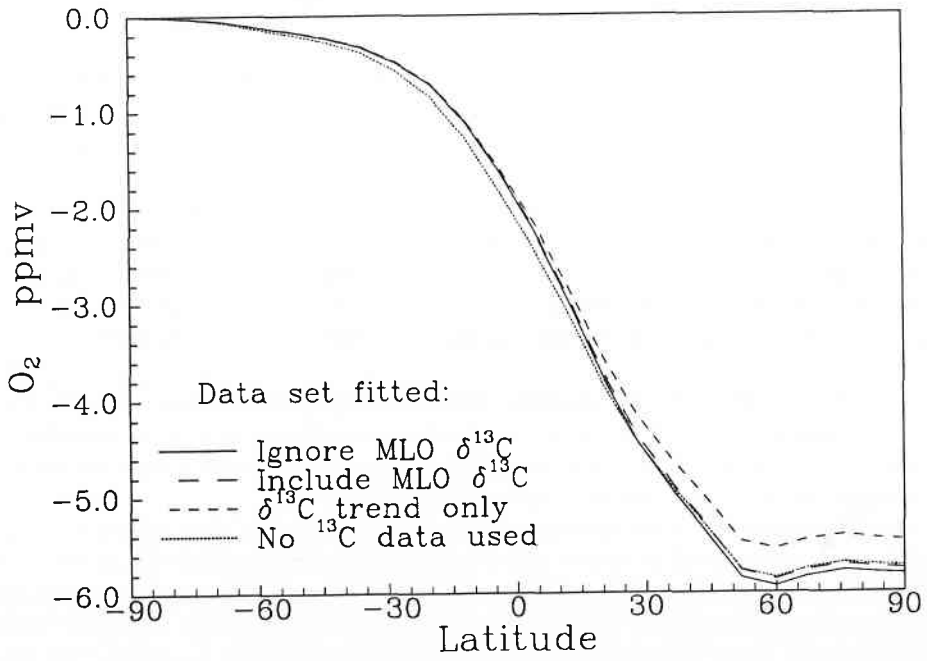

Figure 7: Interhemispheric gradient of oxygen (plotted relative to the South Pole) implied by the estimated source distributions for the same 4 cases as Figure 5. These estimates omit the contributions from marine productivity and have an incomplete representation of the effects of CO production on the oxygen distribution.

Probably the most important new process is the oxygen release from the marine biota. The low solubility of oxygen relative to CO_2 means that seasonal variations in marine productivity give an atmospheric oxygen signal that is much larger than the atmospheric CO_2 signal from marine productivity. Similarly, the spatial gradient in mean production will affect the spatial gradient of oxygen concentrations. The analogy with $\delta^{13}C$ suggests that the most important aspect of oxygen data for constraining the atmospheric carbon budget would be the long-term trend. This implies the need for high quality standards.

Figure 7 shows the inter-hemispheric gradient for oxygen predicted on the basis of the estimated sources for the same 4 cases as shown in Figure 6. These calculations are incomplete since we would expect an additional component to the gradient, arising from the effect of seasonal variations in transport acting on the strong seasonal cycle from marine production as well as the direct effect of annual mean marine production. The prediction in Figure 7 also neglects the complexities arising from the oxidation of those components that pass through CO.

These results indicate that once the CO_2 distribution has been fitted, the spatial gradient of oxygen provides very limited discrimination between alternative budgets; even though the four cases shown have total ocean sinks ranging from 0.96 to 2.05 Gt C y^{-1}, the oxygen profiles are very similar. On the other hand, this similarity means that departures from these curves can be interpreted in terms of marine production with little ambiguity.

7. Concluding remarks

Tables 4, 5, 6 and 7 present a wide range of estimates of the atmospheric CO_2 budget. Our preferred estimate is the final column of Table 7. As noted above, the least-squares estimate is a compromise between data sets that appear to imply distinct pictures of the carbon budget. In this regard it seems worth noting the comments of Claerbout and Muir (quoted by Tarantola, 1987) comparing least squares (ℓ_2 norm) with robust approaches (ℓ_1 norm): *When a traveler reaches a fork in the road, the ℓ_1 norm tells him to take either one way or the other, but the ℓ_2 norm instructs him to head off into the bushes.*

The significance of our estimates of the atmospheric budget can be assessed by comparison with similar estimates compiled in Table 8.

Ref	Year	Fossil	Ocean	Biota	Oc(N)	Oc(T)	Oc(S)	Clear	Fert
IPCC	80–90	5.4	−2.0	?	—	—	—	1.6	?
ΔIPCC	80–90	±0.5	±0.8	—	—	—	—	±1.0	—
KPH	62	2.66	−1.39	0.27	−2.20	1.78	−0.96	1.69	−1.43
KPH	68	3.51	−1.62	0.13	−1.84	1.00	−0.78	1.73	−1.60
KPH	80	5.30	−2.22	−0.31	−2.54	1.28	−0.96	1.79	−2.10
KPH	84	5.19	−2.30	−0.46	−2.30	1.11	−1.10	1.81	−2.27
KPH*	80	5.30	−2.4	0.7	−2.46	1.14	−0.93	2.8	−2.1
TFT	80–7	5.30	−0.4	−1.9	−0.6	1.3	−1.1	1.4	−3.3
S&S	80–7	5.3	−1.7	−0.4	−0.38	−0.48	−0.83	—	—
ΔS&S	80–7	—	±0.7	±0.7	—	—	—	—	—
Quay	70–90	5.1	−2.0	−0.2	—	—	—	—	—
Tab7	86–7	5.4	1.4	−1.0	−2.0	2.5	−2.0	1.1	−2.2
ΔTab7	86–7	±0.3	±1.0	±1.0	—	±0.8	—	±0.8	±0.8

Table 8: Comparison of atmospheric carbon budgets. Units are Gt C y^{-1}. The lines denoted Δ give the ranges of uncertainty (if available) of the values in the preceding line. IPCC refers to IPCC (1990), KPH to Table 10 (and Figures 68 to 71) of Keeling et al. (1989b), KPH* to the last line of Table 7 of Keeling et al. (1989b) where the budget is adjusted to match the short-term increase, TFT to scenario 7 of Tans et al. (1990a), S&S to Sarmiento and Sundquist (1992). The TFT budget is a CO_2 flux budget, the KPH budgets have their totals determined as storage budgets with the regional distribution corresponding to CO_2 fluxes. The IPCC budget is apparently meant to refer to carbon storage as is the S&S budget. The regional distribution of 'ocean storage' in the S&S budget refers to the estimated difference between present and pre-industrial air-sea fluxes. The budget in the last two lines is the CO_2 flux budget from the final column of Table 7 and is balanced with a 0.89 Gt C y^{-1} contribution from CO.

In comparing these budgets, we need to keep in mind the distinctions between CO_2 fluxes, carbon fluxes and carbon storage as described in Section 3c. The Tans et al. (1990) budget was in terms of CO_2 fluxes which were deduced from a combination of inversions of CO_2 data and ocean p_{CO2} data. The Sarmiento and Sundquist budget is an estimate of carbon storage, constructed from the estimate given by Tans et al. (1990a) supplemented by three terms described as corrections: (a) the effect of ocean surface skin temperatures

on p_{CO2}, (b) the transport of atmospheric carbon as CO, and (c) the transport of carbon through rivers. Of these terms, we would regard only the skin temperature effect (Robertson and Watson, 1992) as a genuine correction to the CO_2 fluxes estimated by Tans et al. The other two terms are those that convert CO_2 fluxes to carbon fluxes (the CO term) and then carbon fluxes to carbon storage (the river carbon term). As noted in Section 4d, the analysis by Quay et al. (1992) represents an attempt at obtaining a budget of ocean carbon storage directly.

The budgets presented by Keeling et al. (1989b) are more difficult to assess. The partition of net fluxes between reservoirs is derived from a global carbon cycle model and so presumably reflects carbon storage. The spatial distribution of fluxes is obtained by fitting atmospheric CO_2 data and so presumably reflects CO_2 fluxes. This lack of internal consistency in the Keeling et al. budgets precludes comparison with other estimates.

In assessing the results of our inversion calculations it is important to keep in mind the results of Section 4d and the comparisons between the columns in Table 5. On a global scale, the relative roles of the oceans and biota as sinks of anthropogenic CO_2 are determined primarily by the atmospheric CO_2 and $^{13}CO_2$ budgets. The spatial distributions play a lesser role in constraining the possibilities. Essentially the same conclusion results from the analysis by Enting (1992) using a regional decomposition (as opposed to a process-based decomposition) incorporating inversion results from two-dimensional modelling.

Our posterior estimates of the uncertainties in the sources are derived from *a priori* estimates of the uncertainty in the data. Our results that show the estimates varying within roughly the range of our quoted uncertainties as we make changes in the choice of data set indicates that our error estimates are realistic. This could be investigated further by comparing our *a priori* estimates to estimates obtained by the 'jack-knife' procedure which considers the spread of estimates based on different subsets of the data.

Consequently, the precision to which the atmospheric carbon budget can be determined will depend critically on the precision with which the atmospheric $^{13}CO_2$ budget can be established. Progress in this area will require a more precise knowledge of the isotopic disequilibrium effects of the biota and more importantly, the oceans.

The spatial distributions, as interpreted by transport modelling, serve to resolve the relative contributions of the various ocean regions and the various processes that comprise the net biotic flux. The results in Tables 5, 6 and 7 show consistent regional patterns of ocean releases. Even in cases with quite different global budgets, the differences arise from a combination of relatively small changes in the regional components. In part this reflects the fact that the net air-sea CO_2 flux is the sum of regional contributions of both signs and so the proportional error in the sum can be much greater than in the components. Thus the strengths of atmospheric transport modelling will be in constraining regional sources, for example in investigating possibilities such as the carbon release from tundra proposed by Oechel et al. (1993). The present analyses seem to clearly identify the North Atlantic as a CO_2 sink and the North Pacific as being most likely a CO_2 source. At high southern latitudes, the ocean is a CO_2 source while at mid southern latitudes the oceans are sinks. The equatorial oceans appear as a stronger source than estimated in other studies but a value 30% higher than the prior which was based on p_{CO2} data is not unreasonable.

A corresponding decomposition of biotic CO_2 fluxes will require a disaggregated representation of the biota. Such disaggregation will lead to larger (and more realistic) values for the ranges of uncertainty that apply to the regional air-sea fluxes. This work is currently in progress.

Acknowledgements

The atmospheric transport model was kindly provided by Dr. I.Y. Fung of NASA Goddard Institute of Space Sciences and implemented at CSIRO by Dr. J.V. Mansbridge. The CSIRO transport modelling project is funded by the State Electricity Commission of Victoria. The authors wish to thank Dr. P.P. Tans for supplying a copy of his 1993 paper prior to publication and Dr. I.Y. Fung for stimulating discussions and L.P. Steele, I. Galbally, G. Pearman and C. Mitchell for valuable comments on the manuscript.

References

Azevedo, A.E. 1982. *Atmospheric Distribution of CO_2 and its Exchange with the Biosphere and the Oceans.* Ph.D. Thesis, Columbia University, New York.

Broecker, W.S., Peng, T.-H. and Engh, R. 1980. Modeling the carbon system. *Radiocarbon*, **22**, 565–598.

Brown, M.K.M. 1992. An inversion algorithm for source gases using Green's functions. (Abstract). *Eos Trans. AGU 93*, Fall Meeting Suppl. 94.

Brown, M. 1993. Deduction of emissions of source gases using an objective algorithm and a chemical transport model *J. Geophys. Res.*, , (in press).

CDIAC 1991. *Trends 91: A Compendium of Data on Global Change.* Ed. T.A. Boden, R.J. Serpanski and F.W. Stoss. (Carbon Dioxide Information Analysis Center: Oak Ridge).

Conway, T.J. and Tans, P. 1990. *Atmospheric CO_2 concentrations — The NOAA/GMCC flask sampling network.* NDP—005/R1. (Carbon Dioxide Information Analysis Center: Oak Ridge).

Emanuel, W.R., Killough, G.E.G. and Olson, J.S. 1981. Modelling the circulation of carbon in the world's terrestrial ecosystems. pp 335–364 of *Carbon Cycle Modelling. SCOPE 16.* Ed. B. Bolin. (Wiley: Chichester).

Enting, I.G. 1992. *Constraining the Atmospheric Carbon Budget: A Preliminary Assessment.* Division of Atmospheric Research Technical Paper No. 25. (CSIRO, Australia).

Enting, I.G. 1993. CO_2-climate feedbacks: aspects of detection. In *Feedbacks in the Global Climate System: Will the Warming Speed the Warming?* (Proceedings of IPCC workshop, Woods Hole, October 1992). Ed. G.M. Woodwell (Oxford University Press) (in press).

Enting, I.G. and Manning, M.R. 1989. The seasonal cycle of CO_2 at Mauna Loa: a reanalysis of a digital filtering study. pp124–131 of *The Statistical Treatment of CO_2 Data Records.* Ed. W.P. Elliott. NOAA Technical Memorandum ERL ARL-173. (NOAA, US. Dept. Commerce: Washington).

Enting, I.G. and Mansbridge, J.V. 1989. Seasonal sources and sinks of atmospheric CO_2: Direct inversion of filtered data. *Tellus*, **41B**, 111–126.

Enting, I.G. and Mansbridge, J.V. 1991. Latitudinal distribution of sources and sinks of CO_2: Results of an inversion study. *Tellus*, **43B**, 156–170.

Enting, I.G. and Newsam, G.N. 1990. Inverse problems in atmospheric constituent studies: II. Sources in the free atmosphere. *Inverse Problems*, 6, 349–362.

Enting, I.G. and Pearman, G.I. 1993. Average global distributions of CO_2. In: *The Global Carbon Cycle: Proceedings of the NATO ASI at Il Ciocco, Italy, September 1991.* Ed. M. Heimann (Springer-Verlag) (in press).

Enting, I.G. and Trudinger, C.M. 1993. Modelling studies of small-scale variability in atmospheric CO_2. In *Baseline Atmospheric Program (Australia) 1990.* Ed. S.R. Wilson and J. Gras. (Dept. of Admin. Services and CSIRO: Australia) (in press).

Etcheto, J., Boutin, J. and Merlivat, L. 1991. Seasonal variation of the CO_2 exchange coefficient over the global ocean using satellite wind speed measurements. *Tellus*, **43B**, 247–255.

Francey, R.J. and Goodman, H.S. 1986: Systematic error in, and selection of, insitu $\delta^{13}C$. *Baseline Atmospheric Program (Australia) 1983–84.* Eds. R.J. Francey and B.W. Forgan. (Department of Science, Bureau of Meteorology/CSIRO, Division of Atmospheric Research: Australia) pp 27 –36.

Francey, R.J. and Goodman, H.S. 1988. The DAR stable isotope reference scale for CO_2. *Baseline Atmospheric Program (Australia) 1986.* Ed. B.W. Forgan and P.J. Fraser. (Department of Science and CSIRO: Australia) pp 40–46.

Francey, R.J., Robbins, F.J., Allison, C.E. and Richards, N.G. 1990. The CSIRO global survey of CO_2 stable isotopes. pp 16–27 of *Baseline Atmospheric Program (Australia) 1988.* Ed. S.R. Wilson and G.P Ayers. (Dept. of Admin. Services and CSIRO: Australia).

Friedli, H., Lotscher, H., Oeschger, H., Siegenthaler, U. and Stauffer, B. 1986. Ice core record of the $^{13}C/^{12}C$ ratio of atmospheric CO_2 in the past two centuries. *Nature*, **324**, 237–238.

Fung, I., Prentice, K., Matthews, E., Lerner, J. and Russell, G. 1983. Three-dimensional tracer model study of atmospheric CO_2: response to seasonal exchanges with the terrestrial biosphere. *J. Geophys. Res.*, **88C**, 1281–1294.

Fung, I., John, J., Lerner, J., Matthews, E., Prather, M., Steele, L.P. and Fraser, P.J. 1991. Three-dimensional model synthesis of the global methane cycle. *J. Geophys. Res.*, **96D**, 13033–13065.

Gifford, R.M. 1993. Implications of CO_2 effects on vegetation for the global carbon budget. In: *the Global Carbon Cycle: Proceedings of the NATO ASI at Il Ciocco, Italy, September 1991.* Ed. M. Heimann (Springer-Verlag) (in press).

GMCC 1988. Geophysical Monitoring for Climatic Change. No. 16. Summary Report 1987. Ed. B. Bodhaine and R.M. Rosson. (U.S. Dept. Commerce: Washington).

Hartley, D.E. 1992. *Deducing Trace Gas Emissions Using an Inverse Method in Three-dimensional Chemical Transport Models.* Ph. D. Thesis. MIT. Report No. 17. (Centre for Global Change Science, MIT: Cambridge, Mass.).

Hartley and Prinn 1992. Deducing trace gas emissions using the Kalman filter in NCAR's CCM2 (Abstract). *Eos Trans. AGU 93*, Fall Meeting Suppl. 93.

Hartley, D. and Prinn, R. 1993. On the feasibility of determining surface emissions of trace gases using an inverse method in a three-dimensional chemical transport model. *J. Geophys. Res.*, , (in press).

Heimann, M. and Keeling, C.D. 1989. A three-dimensional model of atmospheric CO_2 transport based on observed winds: 2. Model description and simulated tracer experiments. *Aspects of Climate Variability in the Pacific and Western Americas.* Geophysical Monograph 55. Ed. D.H. Peterson. (AGU: Washington).

Houghton, R.A. 1993. Changes in terrestrial carbon over the last 135 years. In: *the Global Carbon Cycle: Proceedings of the NATO ASI at Il Ciocco, Italy, September 1991.* Ed. M. Heimann (Springer-Verlag) (in press).

Houghton, R.A., Hobbie, J.E., Melillo, J.M., Moore, B., Peterson, B.J., Shaver, G.R. and Woodwell, G.M. 1983. Changes in the carbon content of terrestrial biota and soils between 1860 and 1980: A net release of CO_2 to the atmosphere. *Ecol. Monog.*, **53**, 235–262.

Houghton, R.A., R.D. Boone, J.R. Fruci, J.E. Hobbie, J.M. Melillo, C.A. Palm, B.J. Peterson, G.R. Shaver, G.M. Woodwell, B. Moore, D.L. Skole. and N. Myers 1987. The flux of carbon from terrestrial ecosystems to the atmosphere in 1980 due to changes in land use: geographic distribution of the global flux. *Tellus*, **39B**, 122–139.

IPCC 1990. *Climate Change: The IPCC Scientific Assessment.* Ed. J.T. Houghton, G.J. Jenkins and J.J. Ephraums for the Intergovernmental Panel on Climate Change. (Cambridge University Press: Cambridge).

Keeling, R.F. 1988. *Development of an Interferometric Oxygen Analyzer for Precise Measurement of the Atmospheric O_2 Mole Fraction.* Ph. D. Thesis. Harvard.

Keeling, R.F. and Shertz, S.R. 1992. Seasonal and interannual variations in atmospheric oxygen and implications for the global carbon cycle. *Nature*, **358**, 723–727.

Keeling, C.D., Bacastow, R.B., Carter, A.F., Piper, S.C., Whorf, T.P., Heimann, M., Mook, W.G. and Roeloffzen, H. 1989a. A three-dimensional model of atmospheric CO_2 transport based on observed winds: 1. Analysis of observational data. *Aspects of Climate Variability in the Pacific and Western Americas.* Geophysical Monograph 55. Ed. D.H. Peterson. (AGU: Washington).

Keeling, C.D., Piper, S.C. and Heimann, M. 1989b. A three-dimensional model of atmospheric CO_2 transport based on observed winds: 4. Mean annual gradients and interannual variations. *Aspects of Climate Variability in the Pacific and Western Americas.* Geophysical Monograph 55. Ed. D.H. Peterson. (AGU: Washington).

Kohlmaier, G.H., Bröhl, H., Siré, E.O., Plöchl, M., and Revelle, R. 1987. Modelling stimulation of plants and ecosystem response to present levels of excess atmospheric CO_2. *Tellus*, **39B**, 155–170.

Law, R., Simmonds, I. and Budd, W.F. 1992. Application of an atmospheric transport model to high southern latitudes. *Tellus*, **44B**, 358–370.

Liss, P.S. and Merlivat, L. 1986. Air-sea gas exchange rates: Introduction and synthesis. pp113–127 of *The Role of Air-Sea Exchange in Geochemical Cycling.* Ed. P. Buat-Ménard. (Reidel: Dordrecht).

Marland, G., R.M. Rotty, and N.L. Treat 1985. CO_2 from fossil fuel burning : Global distribution of emissions. *Tellus*, **37B**, 243–258.

Matthews, E. 1985. *Atlas of Archived Vegetation Land-use and Seasonal Albedo Data Sets.* NASA Technical Memorandum No. 86199.

Newsam, G.N. and Enting, I.G. 1988. Inverse problems in atmospheric constituent studies: I. Determination of surface sources under a diffusive transport approximation. *Inverse Problems*, **4**, 1037–1054.

Oechel, W.C., Hastings, S.J., Vourlitis, G., Jenkins, M., Riechers, G. and Grulke, N. 1993. Recent change of Arctic tundra ecosystems from a net carbon dioxide sink to a source. *Nature*, **361**, 520–523.

Pearman, G.I. and Hyson, P. 1986. Global transport and inter-reservoir exchange of carbon dioxide with particular reference to stable isotope distribution. *J. Atmos. Chem.*, **4**, 81–124.

Polglase, P.J. and Wang, Y.P. 1992. Potential CO_2-enhanced carbon storage by the terrestrial biosphere. *Aust. J. Botany*, **40**, 641–656.

Prather, M., McElroy, M., Wofsy, S., Russell, G. and Rind, D. 1987. Chemistry of the global troposphere: Fluorocarbons as tracers of air motion. *J. Geophys. Res.*, **92**, 6579–6613.

Press, W.H., Flannery, B.P., Teukolsky, S.A. and Vetterling, W.T. 1986. *Numerical Recipes: The Art of Scientific Computing* (Cambridge University Press).

Prinn, R., Cunnold, D., Rasmussen, R., Simmonds, P., Alyea, F., Crawford, A., Fraser, P. and Rosen, R. 1987. Atmospheric trends in methyl chloroform and the global average for the hydroxyl radical. *Science*, **238**, 945–950.

Quay, P.D., Tilbrook, B. and Wong C.S. 1992. Oceanic uptake of fossil fuel CO_2: Carbon-13 evidence. *Science*, **256**, 74–79.

Robertson, J.E. and Watson, A.J. 1992. Thermal skin effect of the surface ocean and its implications for CO_2 uptake. *Nature*, **358**, 738–740.

Rotty, R.M. 1987. Estimates of seasonal variation in fossil fuel CO_2 emissions. *Tellus*, **39B**, 184–202.

Russell, G. and Lerner, J. 1981. A new finite differencing scheme for the tracer transport equation. *J. Appl. Meteorol.*, **20**, 1483–1498.

Sarmiento, J.L. and Sundquist, E.T. 1992. Revised budget for the oceanic uptake of anthropogenic carbon dioxide. *Nature*, **356**, 589–593.

Surendran, S. and Mulholland, R.J. 1987. Modeling the variability in measured atmospheric CO_2 data. *J. Geophys. Res.*, **92D**, 9733–9739.

Tans, P.P. 1980. On calculating the transfer of carbon-13 in reservoir models of the carbon cycle. *Tellus*, **32**, 464–469.

Tans, P.P. 1981. $^{13}C/^{12}C$ of industrial CO_2. pp127–129 of *Carbon Cycle Modelling. SCOPE 16*. Ed. B. Bolin. (Wiley: Chichester).

Tans, P.P., Conway, T.J. and Nakazawa, T. 1989. Latitudinal distribution of the sources and sinks of atmospheric carbon dioxide derived from surface observations and an atmospheric transport model. *J. Geophys. Res.*, **94D**, 5151–5172.

Tans, P.P., Fung, I.Y. and Takahashi, T. 1990a. Observational constraints on the global atmospheric CO_2 budget. *Science*, **247**, 1431–1438.

Tans, P.P., Thoning, K.W., Elliott, W.P. and Conway, T.J. 1990b. Error estimates of background atmospheric CO_2 patterns from weekly flask samples. *J. Geophys. Res.*, **95D**, 14063–14070.

Tans, P.P., Berry, J.A. and Keeling, R.F. 1993. Oceanic $^{13}C/^{12}C$ observations: A new window on ocean CO_2 uptake. *Global Biogeochemical Cycles*, , (in press).

Tarantola, A. 1987. *Inverse Problem Theory: Methods for Data Fitting and Model Parameter Estimation* (Elsevier: Amsterdam).

Taylor, J.A. 1989. A stochastic Lagrangian atmospheric transport model to determine global CO_2 sources and sinks — a preliminary discussion. *Tellus*, **41B**, 272–285.

Trenberth, K.E. 1981. Seasonal variations in global sea-level pressure and the total mass of the atmosphere. *J. Geophys. Res.*, **86C**, 5238–46.

Wunsch, C. and Minster, J.-F. 1982. Methods for box models and ocean circulation tracers: mathematical programming and non-linear inverse theory. *J. Geophys. Res.*, **87**, 5647–5662.

Appendix A: The transport model

The calculations were performed using the GISS tracer transport model described by Russell and Lerner (1981), Fung et al. (1983). We used the 'low-resolution' version with an 8° × 10° grid. A year of 4-hourly-averaged winds and monthly-averaged convection generated by the GISS GCM (running at 4° × 5° resolution) is used to specify the model transport. The model also includes a 'diffusive' transport, as described by Prather et al. (1987).

The GISS model works with tracer masses rather than concentrations. One consequence of this is that even if the model is initialised with constant concentrations, it will generate concentration fluctuations due to truncation errors in the transport scheme. (In addition a somewhat larger fluctuation occurs at day 90 due to the discontinuity in the wind fields.) These fluctuations can be about 0.5% or more of the mean concentration (Enting and Trudinger, 1993). Therefore it is important to subtract an 'offset' concentration and compute with the residuals.

As noted above, for periodic sources a steady-state (i.e. an annually periodic cycle plus a globally uniform trend) is achieved after 3 years. Therefore we use the fourth year's results to define our response functions $R_{\tau\omega\phi}$.

Appendix B: Modelling the isotopic disequilibrium of the biota

In Section 4d, we have noted the importance of the isotopic disequilibrium of the terrestrial biota in interpreting the atmospheric ^{13}C budget. We also noted that the estimate of 12‰ Gt C y^{-1} used by Quay et al. (1992) and adopted for comparison purposes by Tans et al. (1993) seemed too low. In order to refine the estimates we have used the compartment model of the terrestrial biota described by Emanuel et al. (1981) with the atmospheric $\delta^{13}C$ specified by the ice-core data of Friedli et al. (1986).

The biotic model is characterised by 6 reservoirs: the atmosphere (which provides a specified boundary condition), ground vegetation, the non-woody parts of trees, wood, detritus and soils. The 6 reservoirs are characterised by their carbon contents C_j (in Gt C), their ^{13}C contents χ_j expressed as Gt C times the standard ratio, R_{standard}, and the inter-reservoir carbon fluxes $\Phi_{j\leftarrow i}$ in Gt C y^{-1}. The C_j and $\Phi_{j\leftarrow i}$ remain fixed at the values given in Table 9. We model the evolution of the ^{13}C content of the biota.

The equations describing this evolution are

$$\frac{d}{dt}\chi_j = \sum_k \alpha_{jk}\frac{\chi_k}{C_k}\Phi_{j\leftarrow k} - \sum_k \frac{\chi_j}{C_j}\Phi_{k\leftarrow j} \qquad \text{for } j = 2 \text{ to } 6.$$

where $\alpha_{jk} = 1$ unless $k = 1$, $\alpha_{j1} = 0.982$ and the atmospheric ^{13}C:^{12}C ratio χ_1/C_1 is specified from the ice-core data. The system is initialised with $\chi_j = 0.982 \times 0.9936 \times C_j$ and integrated from 1800 to 1990.

The isotopic disequilibrium is given by

$$\left(0.982\frac{\chi_1}{C_1}\Phi_{\mathrm{TOT}} - \sum_{j=2}^{6}\frac{\chi_j}{C_j}\Phi_{1\leftarrow j}\right)$$

	Atmos	Ground veg.	Non-wood	Wood	Detrit.	Soil
C_j	—	69	37	432	81	1121
→ Atmos	—	18	25	14	45	11
→ Ground veg	36	—	0	0	0	0
→ Non-wood	77	0	—	0	0	0
→ Wood	0	0	31	—	0	0
→ Detrit.	0	12	21	15	—	0
→ Soil	0	6	0	2	3	—

Table 9: Characteristics of the biotic model of Emanuel et al. (1981). The C_j are the carbon contents of the reservoirs in Gt C, the remainder of the table holds the inter-reservoir carbon fluxes in Gt C y^{-1}.

where $\Phi_{\mathrm{TOT}} = \sum_j \Phi_{j\leftarrow 1}$.

We represent the ice-core δ^{13}C data as a piece-wise linear function connecting the points (1800, 0.9936), (1840, 0.9936), (1900, 0.9933), (1960, 0.9930), (1980, 0.9924), (1990, 0.9922).

The standard case of the model gives a 1987 disequilibrium of 26.5‰Gt C y^{-1}. For comparison we halved all the fluxes in the model while retaining the same reservoir sizes. The disequilibrium effect was reduced to 19.2‰Gt C y^{-1}.

Appendix C: Notation

a — Area of an ocean region.

$A_{j\mu}$ — Matrix defining the relation between source components and data that are fitted. Equal to response matrix T augmented by an identity matrix in order to fit priors, s_μ, and by additional columns to include 'pseudo-sources' specifying mean levels.

B_{G} — Gross CO_2 flux from the terrestrial biota to the atmosphere.

B_{N} — Net biotic carbon flux to atmosphere.

B_{N}^{+} — Net biotic carbon loss.

c_j — jth item of observational data.

$C(z)$ — Ocean carbon concentration as function of depth.

$\bar{C}$ — Average of $C(z)$.

C_j — Carbon content of biotic reservoir j (Appendix B only).

d_j — Weight for jth item fitted, equal to u_j or v_{j-M}.

D_j — Residual $c_j - \sum_\mu A_{j\mu}\hat{\sigma}_\mu$ for jth observation.

$F_\nu(\mu)$ — Scale factor for the effect of source μ on constituent ν.

$G_\nu(\mu)$ — Scale factor for the effect of source μ on the global trend in constituent ν.

j — Generic index for the data that are fitted.

k — Index for equations to be fitted, range from 1 to $M + N$, i.e. one equation from each data item and one for each prior estimate.

M — Number of observations fitted.

N — Number of real source components.

N' — Number of source components estimated — includes 'pseudo-sources'.

N_a — Atmospheric carbon content in Gt.

$q_{\alpha\mu}$ — Factor defining linear combination of source components — the amount of the μth source in the αth combination, x_α.

$r_{standard}$ — Standard ^{13}C:^{12}C ratio (from PDB) = 0.0112372.

R_a — Atmospheric ^{13}C:C ratio (= $^{13}C/(^{12}C + {}^{13}C)$).

R_m — Mixed layer ^{13}C:C ratio.

$R_{standard}$ — Standard ^{13}C:C ratio = $r_{standard}/(1 + r_{standard})$.

R_{ref} — Reference ^{13}C:C ratio used for defining isotopic anomalies.

$R_{\rho\omega\phi}$ — The atmospheric CO_2 response at location ρ at frequency index ω for a unit source with space-time distribution ϕ.

s_μ — Prior estimate for σ_μ.

S_E — Empirical estimate of regional net sea to air CO_2 flux. Used as prior estimate.

S_N — Net air-sea carbon flux = $\Phi_{am} - \Phi_{ma}$.

S_N^+ — Net ocean carbon uptake.

S^* — Net sea-air ^{13}C flux = $\alpha_{am} R_a \Phi_{am} - \alpha_{ma} R_m \Phi_{ma}$.

S_X — Net sea-air ^{13}C anomaly flux.

t — Time (in years).

T — Mixed layer temperature in degrees Celsius.

$T_{j\mu}$ — Contribution to observation j from source μ.

u_j — Standard deviation of observation c_j.

v_μ — Standard deviation of prior estimate s_μ.

$V_{\mu\eta}$ — Covariance of the estimates $\hat{\sigma}_\mu$ and $\hat{\sigma}_\eta$.

x_α — Linear combination of source components, σ_μ.

X — Isotopic anomaly. $X = ([^{13}C]/R_{ref} - [C]) \times 1000$

z — Ocean depth coordinate.

α_{am} — Kinetic air-sea ^{13}C:C fractionation factor. (The numerical values are taken from ^{13}C:^{12}C fractionation factors because the differences are negligible in the present context).

α_{ma} — Kinetic sea-air ^{13}C:C fractionation factor.

α_{eq} — $= \alpha_{ma}/\alpha_{am}$. Equilibrium ^{13}C:^{12}C partitioning factor for atmosphere and mixed layer.

δ_a — $\delta^{13}C$ of atmospheric CO_2.

δ_b — $\delta^{13}C$ of the terrestrial biota.

δ_{eq} — The $\delta^{13}C$ of ocean water in equilibrium with the atmosphere.

δ_m — $\delta^{13}C$ of inorganic carbon in the ocean mixed layer.

$\delta_{i,j}$ — Kronecker delta: $= 1$ if $i = j$, $= 0$ otherwise.

ϵ_x — $(\alpha_x - 1) \times 1000$. Isotopic shift (in ‰) for process x.

ϵ_b — Isotopic shift for biotic uptake.

κ — Air-sea gas exchange coefficient for CO_2, in mol $m^{-2}y^{-1}\mu atm^{-1}$.

μ — General index for source components

$\nu(j)$ — Constituent index for data item j, indicating whether it refers to CO_2, $^{13}CO_2$ or O_2.

ρ_j — Location index for data item j.

σ_μ — μth source component.

$\hat{\sigma}_\mu$ — Estimate of σ_μ.

$\phi(\mu)$ — Index denoting the space-time distribution of source process μ.

Φ_{am} — Gross air-sea CO_2 flux.

Φ_{ma} — Gross sea-air CO_2 flux.

$\Phi_{i \leftarrow j}$ — Carbon flux from biotic reservoir j to reservoir i (Appendix B).

χ_j — Normalised ^{13}C content of biotic reservoir j (Appendix B).

ω_j — Frequency index for data item j.